Molecular Systems Biology 8; Article number 578; doi:10.1038/msb.2012.12
Citation: ***Molecular Systems Biology* 8: 578**

www.molecularsystemsbiology.com

molecular systems biology

A framework for mapping, visualisation and automatic model creation of signal-transduction networks

Carl-Fredrik Tiger[1,2,8], Falko Krause[2,8], Gunnar Cedersund[1,3,4], Robert Palmér[3], Edda Klipp[2], Stefan Hohmann[1], Hiroaki Kitano[3,5,6,7] and Marcus Krantz[1,2,5,*]

[1] Department of Cell and Molecular Biology, University of Gothenburg, Göteborg, Sweden, [2] Theoretical Biophysics, Humboldt-Universität zu Berlin, Berlin, Germany, [3] Department of Clinical and Experimental Medicine, Diabetes and Integrative Systems Biology, Linköping University, Linköping, Sweden, [4] Freiburg Institute of Advanced Sciences, School of Life Sciences, Freiburg, Germany, [5] The Systems Biology Institute, Tokyo, Japan, [6] Sony Computer Science Laboratories, Inc., Tokyo, Japan and [7] Okinawa Institute of Science and Technology, Okinawa, Japan
[8]These authors contributed equally to this work
* Corresponding author. Theoretical Biophysics, Humboldt-Universität zu Berlin, Invalidenstr. 42, Berlin 10115, Germany. Tel.: +49 30 2093 8389; Fax: +49 30 2093 8813; E-mail: marcus.krantz@biologie.hu-berlin.de

Received 8.7.11; accepted 16.3.12

Intracellular signalling systems are highly complex. This complexity makes handling, analysis and visualisation of available knowledge a major challenge in current signalling research. Here, we present a novel framework for mapping signal-transduction networks that avoids the combinatorial explosion by breaking down the network in reaction and contingency information. It provides two new visualisation methods and automatic export to mathematical models. We use this framework to compile the presently most comprehensive map of the yeast MAP kinase network. Our method improves previous strategies by combining (I) more concise mapping adapted to empirical data, (II) individual referencing for each piece of information, (III) visualisation without simplifications or added uncertainty, (IV) automatic visualisation in multiple formats, (V) automatic export to mathematical models and (VI) compatibility with established formats. The framework is supported by an open source software tool that facilitates integration of the three levels of network analysis: definition, visualisation and mathematical modelling. The framework is species independent and we expect that it will have wider impact in signalling research on any system.
Molecular Systems Biology **8**: 578; published online 24 April 2012; doi:10.1038/msb.2012.12
Subject Categories: metabolic and regulatory networks; computational methods; simulation and data analysis
Keywords: combinatorial complexity; mathematical modelling; network mapping; signal transduction; visualisation

Introduction

All living cells interact with and respond to their environment via the cellular signal-transduction network. This network encompasses all cellular components and processes that are required to receive, transmit and interpret information. Due to its key role in cellular physiology, the signalling network, and several of its subnetworks, have been intensely studied in a range of organisms. However, such networks are highly complex and difficult to analyse due to the so-called combinatorial explosion (Hlavacek *et al*, 2003). This explosion refers to the fact that the specific state of each component is determined by multiple covalent modifications or interaction partners, and that these possibilities rapidly combine to a very large number of possible specific states. Experimental data do not generally distinguish between all these specific states, but instead focus mostly on reactions between pairs of components, usually giving no or limited information on other modifications or interaction partners of the reactants. Hence, there is a discrepancy between the granularity of the empirical data and the highly defined specific states used in most mathematical models. This makes the interpretation and use of empirical data in the context of such model states ambiguous and often arbitrary. These problems pose major challenges for systems biology, as they prevent us from (i) unambiguously describing a network, (ii) visualising it without simplifications or unsupported assumptions and (iii) automatically generating mathematical models from knowledge in data repositories.

Large efforts have been invested in addressing these issues. Signalling systems are commonly visualised through the informal 'biologist's graph' that is simple and intuitive, but lacks the stringent formalism and precision required to meet the three criteria above (exemplified by Thorner *et al*, 2005). The lack of standardised glyphs (defining e.g., mechanism of information transfer and how edges combines to regulate target nodes) makes the information in the 'biologist's graph' ambiguous and difficult to reuse. To address this, the

community has developed the Systems Biology Graphical Notation, SBGN (Le Novere *et al*, 2009). This includes three visual formats; the activity flow diagram, the entity relationship diagram and the process description (or process diagram). The activity flow diagram shares many properties with the 'biologist's graph', but the entity relationship diagram and process description allow precise representations. The process description corresponds to the state transition reaction format used in most models developed by the systems biology community, and which have been standardised in the Systems Biology Markup Language (SBML; Hucka *et al*, 2003). The process description could meet each of the three criteria above but its utility is severely affected by the combinatorial explosion. It is based on a specific state description, which means that, for each component, each possible combination of modifications and interaction partners must be accounted for explicitly. Hence, only very simple systems can be described completely and only very few models include the entire state space (Kiselyov *et al*, 2009) while the vast majority include simplifying omissions. While simplifications are often necessary, the lack of discrimination between arbitrary omissions and exclusions based on experimental evidence is a significant shortcoming. These issues are partially addressed in the entity relationship diagram, or molecular interaction map, which comes in two flavours; explicit and implicit (called heuristic and combinatorial by the author (Kohn *et al*, 2006)). The explicit version requires all specific states to be displayed and hence share the limitations of the process description. In contrast, the implicit version displays only the possible reaction types (or elemental reactions, as we will call them below) and hence largely avoids the combinatorial explosion. The entity relationship diagram represents each component as a single node and reactions in a condensed format. While not as intuitive as the other SBGN formats, it has the advantage of concentrating all information on a given protein and works especially well for simple regulatory circuits, as the concentrated information makes it difficult to trace the order of events in more complex networks. The three SBGN format has complementary strengths, but there is currently no software available for conversion between the three different visualisation formats. However, the SBGN standards are under continuous development and these issues will likely be addressed in the future through the SBGN markup language, SBGN-ML.

Similar efforts on the modelling side have resulted in rule-based modelling and associated visualisation formats (Faeder *et al*, 2005). Briefly, rules are defined as reactions that are valid under a particular set of contingencies, and each reaction is specified for each such contingency set. This means that when a reaction's rate is increased by phosphorylation of one component it will be defined by two rules; one where that component is phosphorylated and one where it is not. While these rules define the entire state space and the system stays subject to the full combinatorial explosion, the rule description has alleviated the combinatorial problem in two respects: (1) the system has been described more compactly and (2) the actualised state space might be significantly reduced by introducing only those states that are actually populated (Lok and Brent, 2005), or by using agent-based stochastic modelling (Sneddon *et al*, 2011). The rule definition format is also a significant step towards the granularity of empirical data, as compared with the abstract-specific states. These advantages are mirrored on the visualisation side by graphical reaction rules, which use the process description format to display individual rules (Blinov *et al*, 2006). Network level visualisation has used either topological contact maps (Danos, 2007) or entity relationship diagrams (Le Novere *et al*, 2009), and these complementary visualisation formats have recently been combined in the extended contact map (Chylek *et al*, 2011). Contact maps have software support, but neither entity relationship diagrams nor extended contact maps can be generated automatically from the rule-based models. Hence, the rule-based format partially addresses the automatic creation of models from data repositories (iii), as it provides the tools to generate mathematical models automatically once the knowledge has been reformulated as rules. However, the rule-based system provides a cumbersome format for (i) unambiguous network description and is not developed for (ii) comprehensive visualisations. Taken together, this raises the question whether graphical- and model-based formats are the most appropriate for stringent network definition, or whether there are more suitable network definition formats that allow both visualisation and automatic model generation.

Here, we present a new framework to describe cellular signal-transduction networks. Our network definition has the same granularity as experimental data, avoids the combinatorial complexity, can be automatically visualised in complementary graphical formats including all three SBGN formats and unambiguously defines mathematical models. The *rxncon* software tool complements the framework by automating visualisation and model creation. The key feature of our framework is the strict separation of elemental reactions (and their corresponding states); which defines the possible signalling events in the network, from contingencies; which describes the contextual constrains on these reactions. Importantly, each elemental reaction corresponds directly to a single empirical observation, such as a protein–protein interaction or a specific phosphorylation. The contingencies define the constraints on these elemental reactions in terms of one or more elemental states, for example, by defining the active state of a protein kinase or the composition of a functional protein complex. Hence, the format directly link model states to empirical observations at the same level of granularity, which pre-empts the need for additional assumptions or extrapolations. Moreover, the separation between reactions and contingencies largely avoids the combinatorial explosion as only combinatorial states with known functional influence are considered. The *rxncon* tool provides automatic export to established visual formats and to two new visualisation methods, which allow compact comprehensive representation. Finally, the framework is stringent and unambiguously defines a mathematical model, and the *rxncon* tool support export to SBML and rule- or agent-based models. This allows coding of models in a format that mirrors empirical data, which can be automatically visualised and which is highly suitable for iterative model building. We illustrate our new approach by conducting the most comprehensive literature survey to date of the complete MAP kinase signalling network of *Saccharomyces cerevisiae*. Taken together, we provide a framework that integrates the three levels of network analysis;

definition, visualisation and mathematical modelling and a supporting software tool for automatic visualisation and export to mathematical models. We expect this to be highly useful for the community and envision a common framework to bridge different standards as well as experimental and theoretical systems biology efforts.

Results

This section describes the architecture of the framework, including its data structure, the different methods of visualisation and how it relates to a mathematical model (Figure 1A). In the first part, we present the results of the methods development and describe the system in detail. In the second part, we present our results using the MAP kinase network. The framework has been implemented in the *rxncon* software tool that is distributed freely under the open source LGPL licence and can be downloaded from www.rxncon.org.

The data structure

The events in a signal-transduction network can be categorised in four types: (1) catalytic modifications, (2) bindings and interactions, (3) degradation and synthesis and (4) changes in localisation. Due to the limited information on spatial (re)distribution of components, we have focused on types 1–3 here (Table I). However, the framework is fully capable to include localisation reactions and the *rxncon* tool will be upgraded to encompass these in the future. The first step of the network definition is to distil the available knowledge into two distinct categories of information: *what* can happen, and *when* it can happen. The *what*-aspect (referred to as C1, or *elemental reactions*) specifies the possible events, including the event type (1–3 above), and which components and sites that are involved. The *when*-aspect (referred to as C2, or *contingencies*) specifies how the reaction rate is affected by the state of the involved components. For instance, the MAP kinase Hog1 phosphorylate its target Hot1 (C1—'what'; Figure 1B), and this reaction only occurs when Hog1 is phosphorylated on both Thr174 and Tyr176 (C2—'when'). This second category of knowledge therefore represents the causal relationships, or *contingencies*, between the *reactions* characterised in the first class of knowledge. The separation of C1 from C2 allows us to define even large complex networks stringently in a concise format, as exemplified with the yeast MAP kinase network below.

The what-aspects of the knowledge are represented in the *reaction list* (Figure 1C; simplified example). Importantly, we have broken down the reaction network in *elemental reactions*, which change *elemental states*. An elemental state is similar to an empirical observation, such as an interaction between two proteins or a specific modification at a specific site on a specific protein. If a protein has been phosphorylated on two sites, this corresponds to two different elemental states. In other words, the elemental states correspond to overlapping (non-disjoint) sets. This is different from the specific states in ordinary state transition models, but analogous to the macroscopic states used in the works by Conzelmann *et al* (2008) (Borisov *et al*, 2008). An elemental reaction is similarly defined as a two-component reaction that modifies a single elemental state. Note that this precludes lumped reactions and that, for example, a kinase–substrate interaction and phosphorylation must be described by two different elemental reactions. Hence, the reaction list has the same granularity as typical empirical data, which pre-empts the need for assumptions in the mapping process. It also allows us to use the established format for high-throughput data (Stark *et al*, 2006), including specific referencing of each reaction with PubMed identifiers and complemented with additional details such as active domains, subdomains and residues (Supplementary Tables S1 and S2).

The when-aspect of the knowledge is described in the *contingency list* (Figure 1D; simplified example). This list defines the contextual constraints on all elemental reactions. Most contingencies will correspond to the direct effect of single elemental states of the components involved in the particular elemental reaction, but *Boolean states* allow for combinatorial effects and indirect effects in, for example, scaffolds that cannot be directly attributed to a single elemental state in one of the reactants. There are six distinct reaction contingencies; the Effector can be absolutely required (!), positive (K+), completely neutral (0), negative (K−), absolutely inhibitory (x) or of unknown effect (?). These overlap partially with the influences of entity relationship diagrams (Le Novere *et al*, 2011), but distinguish between no effect (0) and no known effect (?). The Boolean states provide a middle layer between reaction contingencies and a combination of elemental states and/or inputs, using either 'AND' or 'OR' to define, for example, large complexes or alternative mechanisms. In addition, *inputs* and *outputs* function as elemental states and reactions, respectively, at the interface between the network and the external environment. Each row in the contingency list contains a Target (elemental reaction, output or Boolean state), an Effector (elemental state, input or Boolean state) and a symbol describing how the Effector influences the Target (Contingency) that is a contingency symbol (!, K+, 0, K−, x, ?) when the Target is an elemental reaction or an output and a Boolean operator (AND, OR) when the Target is a Boolean state. The data structure is illustrated with a simplified version of the Sho branch of the HOG pathway (Figure 1B). The reaction list state that, for example, Hog1 phosphorylates ('P+') Hot1 (Figure 1C; eighth reaction; on the last row), and the contingency list state that this reaction requires ('!') that Hog1 is phosphorylated on both Thr174 and Tyr176 (Figure 1D, last two rows). These states in turn correspond to the reactions six and seven, respectively (Figure 1C). Hence, the reaction and contingency information suffice to describe the network and their separation keeps the description concise and at the granularity of empirical data. Consequently, the data structure addresses the first issue; unambiguous network definition.

Visualising the signal-transduction network

We address the second issue; comprehensive visualisation, with two novel forms of visualisation; the *contingency matrix* and the *regulatory graph*. These also keep reactions and contingencies separate and hence avoid the combinatorial

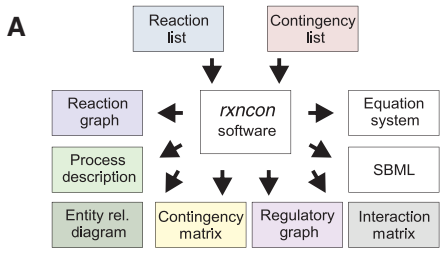

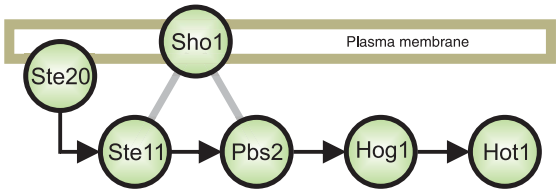

C Reaction list

Comp. A	Re. type	Comp. B	Reaction	State
Sho1	ppi	Ste11	Sho1_ppi_Ste11	Sho1–Ste11
Sho1	ppi	Pbs2	Sho1_ppi_Pbs2	Sho1–Pbs2
Ste20	P+	Ste11	Ste20_P+_Ste11	Ste11-P
Ste11	P+	Pbs2_[S514]	Ste11_P+_Pbs2_[S514]	Pbs2_[S514]-P
Ste11	P+	Pbs2_[T518]	Ste11_P+_Pbs2_[T518]	Pbs2_[T518]-P
Pbs2	P+	Hog1_[T174]	Pbs2_P+_Hog1_[T174]	Hog1_[T174]-P
Pbs2	P+	Hog1_[Y176]	Pbs2_P+_Hog1_[Y176]	Hog1_[Y176]-P
Hog1	P+	Hot1	Hog1_P+_Hot1	Hot1-P

D Contingency list

Target	Cont.	Effector
Ste20_P+_Ste11	+	Sho1–Ste11
Ste11_P+_Pbs2_[S514]	+	Sho1–Pbs2
Ste11_P+_Pbs2_[S514]	+	Sho1–Ste11
Ste11_P+_Pbs2_[S514]	!	Ste11-P
Ste11_P+_Pbs2_[T518]	+	Sho1–Pbs2
Ste11_P+_Pbs2_[T518]	+	Sho1–Ste11
Ste11_P+_Pbs2_[T518]	!	Ste11-P
Pbs2_P+_Hog1_[T174]	!	Pbs2_[S514]-P
Pbs2_P+_Hog1_[T174]	!	Pbs2_[T518]-P
Pbs2_P+_Hog1_[Y176]	!	Pbs2_[S514]-P
Pbs2_P+_Hog1_[Y176]	!	Pbs2_[T518]-P
Hog1_P+_Hot1	!	Hog1_[T174]-P
Hog1_P+_Hot1	!	Hog1_[Y176]-P

E Contingency matrix

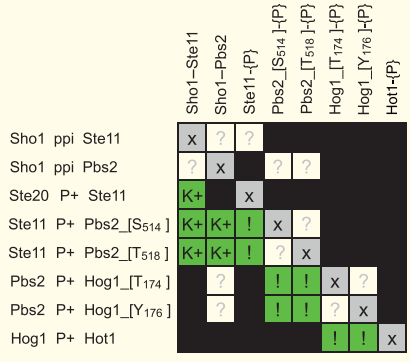

F Reaction graph

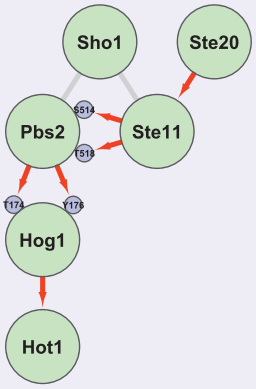

G Regulatory graph

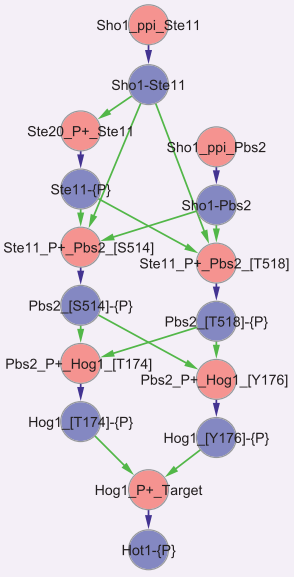

H Limited process description

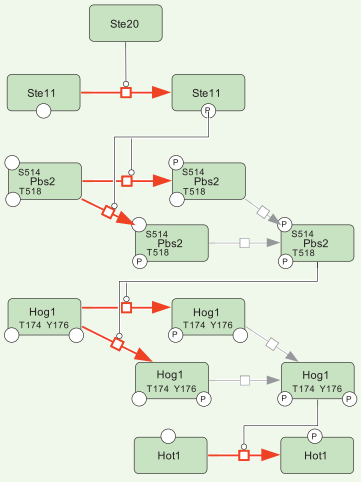

I Interaction/distance matrix

	Sho1	Ste20	Ste11	Pbs2	Hog1	Target
Sho1	–	–	ppi	ppi	–	–
Ste20	–	–	P+	–	–	–
Ste11	ppi	–	–	P+	–	–
Pbs2	ppi	–	–	–	P+	–
Hog1	–	–	–	–	–	P+
Hot1	–	–	–	–	–	–

	Sho1	Ste20	Ste11	Pbs2	Hog1	Target
Sho1	2	–	1	1	2	3
Ste20	2	–	1	2	3	4
Ste11	1	–	2	1	2	3
Pbs2	1	–	2	2	1	2
Hog1	–	–	–	–	–	1
Hot1	–	–	–	–	–	–

J Entity relationship diagram

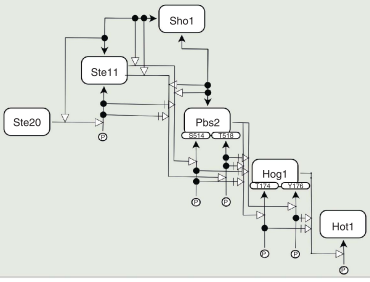

explosion and implicit assumptions. Both include the complete information about reactions (C1) and contingencies (C2). This data structure is also well suited for visualisation in entity relationship diagrams or extended contact maps, and the *rxncon* software tool supports export to the entity relationship format (Chylek *et al*, 2011; Le Novere *et al*, 2011). We also provide export to the reaction graph/activity flow diagram and the process description, though neither of these can fully and accurately represent the network as discussed below. Nevertheless, they all provide their unique advantages and can be automatically generated with the *rxncon* tool and the information in the reaction and contingency lists.

The contingency matrix integrates the information in the reaction and contingency lists (Figure 1E). The matrix is spanned by the reactions and their corresponding states (C1) and populated by the contingencies of reactions on states (C2). Each row corresponds to one elemental reaction and each column corresponds to one elemental state. The symbol in each reaction–state intersection specifies how that specific reaction depends on that specific state. Together, one row contains the complete set of rules a reaction follows, and hence describes how it works in every specific state. This is related to a dependency matrix (Yang *et al*, 2010), although the entries in the contingency matrix are more detailed and unambiguous. In the example (Figure 1E), the first row shows that (a) the binding of Sho1 to Ste11 cannot occur if either of the components is already part of such a dimer (column 1), (b) that we do not know whether the prior binding of Sho1 to Pbs2 (column 2) or phosphorylation of Ste11 (column 3) effects the Sho1–Ste11 binding and (c) that the other states appearing in the row are irrelevant for this specific binding reaction—as they do not describe properties of Sho1 or Ste11. The primary advantages of the contingency matrix are that it (1) allows a comprehensive documentation/visualisation of all reactions and dependencies within the network, (2) that it does so without requiring assumptions, (3) that it explicitly defines unknowns and hence gaps in our knowledge and (4) that the matrix constitutes a template from which mathematical models can be derived automatically (see below).

Table I Thirteen reaction types were used to map the MAP kinase network

Reaction	Category type	Category	Subclass ID	Subclass	Modifier or boundary	Reaction type ID	Reaction name
P+	1	Covalent modification	1.1	(De)Phosphorylation	P	1.1.1	Phosphorylation
P−	1	Covalent modification	1.1	(De)Phosphorylation	P	1.1.2	Dephosphorylation
AP	1	Covalent modification	1.1	(De)Phosphorylation	P	1.1.3	Autophosphorylation
PT	1	Covalent modification	1.1	(De)Phosphorylation	P	1.1.4	Phosphotransfer
GEF	1	Covalent modification[a]	1.2	GTP/GDP hydrolysis/ exchange	P	1.2.1	Guanine Nucleotide Exchange
GAP	1	Covalent modification[a]	1.2	GTP/GDP hydrolysis/ exchange	P	1.2.2	GTPase Activation
Ub+	1	Covalent modification	1.3	(De)Ubiquitination	Ub	1.3.1	Ubiquitination
CUT	1	Covalent modification	1.4	Proteolytic processing	Truncated	1.4	Proteolytic cleaveage
ppi	2	Association	2.1	ppi	N/A	2.1.1	Protein–protein interaction
ipi	2	Association	2.1	ipi		2.1.2	Intra-protein interaction
i	2	Association	2.2	i	N/A	2.2	Interaction (non-proteins)
BIND	2	Association	2.3	BIND	N/A	2.3	Binding to DNA
DEG	3	Synthesis/degradation	3.3	DEG	N/A	3.3	Degradation

The table indicates reaction type and classification. Additional details are provided in the 'Reaction Definition' sheet of Supplementary Tables S1 and S2.
[a]For convenience, the G-protein cycle is approximated as a covalent modification by addition/removal of phosphate to/from a basic, GDP-bound form.

Figure 1 Schematic representation of the data structure. (**A**) The input data are the reaction and contingency lists, which contains the 'what-aspects' and 'when-aspects' of the reaction network, respectively. The *rxncon* software uses these lists to create a range of visualisations as well as computational models. These conversions require no additional information and are fully automated. (**B**) A simplified version of the Sho1 branch of the Hog pathway in *S. cerevisiae* will be used to illustrate the data structure. This 'biologist's graph' shows the activating phosphorylation cascade (arrows) from Ste20 to Hot1. Scaffolding and membrane recruitment by Sho1 facilitates the first two phosphorylation events (grey lines). (**C**) The (simplified) reaction list defines the elemental reactions between pairs of components. It includes the two components (columns I and III), reaction type (column II; 'ppi' = protein–protein interaction, 'P+' = phosphorylation; see Table I for complete list of reactions), reaction (column IV, a concatenation of the components and the reaction type) and resultant state (column V; protein dimers or phosphorylated states). Note that each elemental state only defines a single aspect of each component's specific state. (**D**) The (simplified) contingency list defines the relationship between states and reactions. It contains the affected reaction (Target, column I), the influencing state (Effector, column III), and the effect this particular state has on that reaction (contingency, column II). (**E**) The reaction and contingency information is summarised in the contingency matrix. The matrix is defined by elemental reactions (rows) and states (columns). The cells define how (if) each reaction (row) is affected by each state (column); that is, the reactions' contingencies on different states. Note that only direct contingencies are considered; reaction/state intersections which do not share components are blacked out. The grey fields ('x') are automatic as states are binary and hence a reaction cannot occur if the state is already true. The green fields ('!'/'K+') are imported from the contingency list, and all other open fields are defined as unknown effect ('?'). This information can also be visualised in a number of graphical forms: The reaction graph (**F**) displays network topology with either components or their domains as functional units. The regulatory graph (**G**) combines the reaction and contingency information to display the causal relationship between the reactions in the network and provides a complete graphical representation of the knowledge compiled in the contingency matrix. The limited process description (**H**) displays the catalytic modifications in the signal-transduction network as state transitions with catalysts but without complex formation (compare Supplementary Figure S1). The interaction and distance matrices (**I**) provide a compact description of network topology and allow calculation of distances between nodes. Finally, the reaction and contingency data can be visualised as an entity relationship diagram (**J**). These visualisations and the equation system for this system, subsystem or your own favourite network defined in the same format can be automatically generated using the *rxncon* software.

The *reaction graph* displays a topological, directed reaction network (Figure 1F). It represents each entity as a single node and each relationship between a pair of entities as a single edge. Edges can be non-directional (e.g., protein – protein interaction), unidirectional (e.g., phosphorylation) or bidirectional (e.g., phosphotransfer). The full reaction graph displays the domains and residues involved in each reaction. The protein parts are independent nodes and defined as neighbours (proteins can have domains or residues, domains can have subdomains or residues, subdomains can have residues). The inclusion of domain information makes the reaction graph similar to the (extended) contact maps (Danos, 2007; Chylek *et al*, 2011). The reaction graph and contact maps are both purely topological and do not include any contextual information, in contrast to the extended contact map which, for example, may show that binding only occurs to phosphorylated residues. We also use a condensed variant that displays only the central node for each component and collapses multiple reactions of the same kind between a pair of components to a single edge, and hence corresponds closely to the activity flow diagram of SBGN (Supplementary Figure S1B; Le Novere *et al*, 2009). The advantages of the reaction graph are (1) the relative simplicity that makes it useful for visualisation of even large networks and (2) that it is suited for visualisation of large-scale data sets within the context of that network (see below).

The *regulatory graph* shows how information is conveyed through the network (Figure 1G). It improves on the reaction graph by including information on causality between the reactions in the network (C2 data). The regulatory graph shows the network's regulatory structure; that is, which reactions (via states) actually influence the rate of other reactions. It is a bipartite graph with the elemental reactions (red) and elemental states (blue) as nodes. Reaction-to-state edges simply show which reactions produce or consume which states. The state-to-reaction edges show which states (products of upstream reactions) affect the dynamics of which (downstream) reactions. These state-to-reaction edges correspond to the symbols in the contingency list, i.e., '!', 'K + ', 'K – ' or 'x'. The regulatory graph can easily be translated into an influence graph, which can be used for structural analysis of the network (Kaltenbach *et al*, 2011). In contrast to the influence graph or 'story' (Danos, 2007), the regulatory graph strictly separates the effects of reactions (production or destruction of states) and the modifiers (increase or decrease in reaction rates) via distinct edge types. Furthermore, only the (modified) elemental states are displayed and the (the unmodified) complementary source/target state is implicit. Hence, like in the 'stories', cyclic motifs only appear when there is a true feedback in the system. This visualises both the (possible) sequence of events and the feedbacks clearly. However, in contrast to the 'story', the regulatory graph is comprehensive and simultaneously visualises all possible paths or 'stories'. In this example (Figure 1G), the uppermost node pair corresponds to the reaction where Sho1 binds Ste11 (Sho_ppi_Ste11) and the resulting state Sho1–Ste11. The reaction-to-state edge linking these two nodes identifies Sho1–Ste11 as the product of this binding reaction. Note that the source states for this reaction are omitted (i.e., Sho1 not bound to Ste11 and Ste11 not bound to Sho1). The state-to-reaction edge from Sho1–Ste11 to Ste20_P + _Ste11 shows that the phosphorylation of Ste11 by Ste20 is enhanced in the Sho1–Ste11 complex. This reaction in turn produces the state Ste11-{P}, which is required for phosphorylation of Pbs2 on both Ser514 and Thr518. Hence, the information flow can be followed throughout the network as all edges are unidirectional. The main advantages of the regulatory graph are that it (1) allows a comprehensive documentation/visualisation of all reactions and contingencies within the network, (2) that it does so in a very compact format (3) without forcing non-supported assumptions, (4) that it can be used for structural analysis of the network and (5) that it clearly shows the information flow through the network.

Process descriptions are well established and allow visualisation of the information flow and mechanistic detail simultaneously (Kitano *et al*, 2005). They are excellent for representation of small networks which are completely known, but lack of data (of the right granularity) invariably lead to unsupported assumptions. In addition, these diagrams rapidly become very complex, generally forcing *ad hoc* reduction and additional implicit and unsupported assumptions. Therefore, process descriptions do not allow a complete description of the network with the stringency we require. However, the process description can be clear and easy to read, and we generate a limited version which excludes complex formation and hence avoids most of the combinatorial complexity. The difference is highlighted by the upper three nodes in the example (Figure 1H), where Ste20 phosphorylates Ste11. In contrast to full process description, the binding of Ste11 to Sho1, and how this binding would affect the phosphorylation, is not included (compare Supplementary Figure S1). The (limited) process description has several advantages: It (1) is intuitive to read and (2) defines in which internal state(s) an enzyme is active, its substrate and the exact target residue, which (3) conveys the information flow through the pathway, the enzyme–substrate relationships as well as the gaps in our understanding of these aspects.

The information can also be used to generate interaction matrices that specify which components react with which components. These can be rendered at several levels of detail ranging from a complete interaction matrix including protein domains and target residues that defines each interaction type, via condensed interaction matrices with only one row and column per protein that still contains reaction type information (Figure 1I, upper matrix), to numerical matrices that only include information on connection and directionality. We used the latter to calculate the distances within the network to generate a distance matrix (Figure 1I, lower matrix).

Finally, the *rxncon* tool provides export to entity relationship diagrams (Figure 1J). Like the regulatory graph, the entity relationship diagram displays reactions and contingencies separately and hence largely avoids the combinatorial complexity. The entity relationship diagram has the advantage of concentrating all information on a given protein around a central node, which works especially well for simple regulatory circuits. This emphasises the role of each component within the network, in contrast to the regulatory graph which emphasises the information flow through the network. The entity relationship diagram is generated automatically by the

rxncon software and visualised via Biographer (Biographer). In the same way, the *rxncon* software can be used to generate the contingency matrix, the reaction graphs, the regulatory graph, and, via BioNetGen (Blinov *et al*, 2004), the SBML file that constitute the basis for the process description. These generations are fully automated and hence the framework addresses the issue of (ii) automatic network visualisation without further assumptions and—in the case of the contingency matrix and regulatory graph—without any simplifications.

Generation of mathematical models

The contingency matrix is a template for automatic generation of mathematical models. Each elemental reaction corresponds to a basic (context-free) rule in a rule- or agent-based model (Table II), or, in other words, a set of rules that share a reaction centre (Chylek *et al*, 2011). All contextual constrains on an elemental reaction is defined in a single row in the contingency matrix, and this row defines the elemental reaction's implementation in the rule-based format. The basic rule suffices if there are no known modifiers of a particular elemental reaction (i.e., only '0' and '?' apart from the intersection with its own state(s) (which is always 'x' for a product state and '!' for a source state)). Every other contingency splits the expression in two rules; one when that elemental state is true and one when it is false. The number of rules needed only increases with the number of quantitative modifiers ('K+' and 'K−') as the qualitative modifiers sets the rate constant to zero in either the 'true' (for 'x') or false (for '!') case (see Supplementary information for details). The expansion to rules is fully defined in our data format and the *rxncon* software tool automatically generates the input file for the computational tool BioNetGen (Blinov *et al*, 2004). This file can be used for rule-based modelling, network-free simulation and creation of SBML files. The translation to and from the rule-based format is unambiguous in both directions, and we illustrate this with translation of a rule-based model of the pheromone response pathway (yeastpheromonemodel.org). This model contains lumped reactions which we translate to combinations of elemental reactions, resulting in a different equation structure but the same functionality given appropriate choice of rate constants (Supplementary Table S3). Furthermore, we cannot distinguish different identical proteins in, for example, homodimers, and can therefore not define strict *trans*-reactions within such dimers. Apart from these issues, we can reproduce the same model with only cosmetic/nomenclature differences (see Supplementary information for details). Hence, the framework addresses the issue of (iii) automatic model generation from the database of biological information.

Mapping the MAP kinase network

As a benchmark, we have used the presented framework and an extensive literature search to create a comprehensive map for the yeast MAP kinase network (Supplementary Table S1). Reactions have been defined with specific residues and domains whenever experimental support was sufficient. The degree of experimental evidence has been evaluated manually and individually for each entry, and references to primary research papers supporting each interaction have been included in the reaction and contingency lists (column 'PubMedIdentifier(s)'). We have used mechanistic data on reactions (C1) and a combination of mechanistic and genetic data on contingencies (C2) between reactions and reactants' states from primary research literature. The mapping is based solely on primary research papers and *de facto* shown data to ensure a high-quality network reconstruction. We chose to exclude almost all genetic data as indirect effects cannot be ruled out even in well-performed genetic screens. Finally, we decided not to include spatial data, as we found information especially on regulation of (re)localisation too sparse. To the best of our knowledge, we have eliminated all questionable information from the compiled data set, and convincing reactions lacking solid mechanistic evidence have been included but clearly and distinctly labelled.

The MAP kinase network contains 84 components, 181 elementary states and 222 elementary reactions, corresponding to many hundreds of thousands of specific states. This network is large enough to be a severe challenge to the established visualisation and analysis methods. We did in fact fail to generate the complete state space and terminated the BioNetGen expansion after the first three iterations which generated 207, 1524 and 372 097 specific states, respectively. We use a range of graphical formats to visualise different aspects of this highly complex network. First, we display the network topology in the *reaction graphs* (Figure 2). These

Table II Implementation of elemental reactions in the rule-based format

Elemental reaction	BioNetGen rule implementation	
Interactions (''ppi'', ''i'' or ''bind'')	A(B) + B(A) <−> A(B!1).B(A!1)	kf, kr
Intra-protein interactions (ipi)	A(A1,A2) <−> A(A1!1,A2!1)	kf
Phosphorylations (P+)	A + B(Psite~U) −> A + B(Psite~P)	kf
Autophosphorylations (AP)	A(Psite~U) −> A(Psite~P)	kf
Phosphotransfers (PT)	A(Psite~P) + B(Psite~U) <−> A(Psite~U) + B(Psite~P)	kf, kr
Dephosphorylations (P−)	A + B(Psite~P) −> A + B(Psite~U)	kf
Nucleotide exchanges (GEF)	A + B(GnP~U) −> A + B(GnP~P)	kf
Nuclease activations (GAP)	A + B(GnP~P) −> A + B(GnP~U)	kf
Ubiquitination (Ub+)	A + B(UBsite~U) −> A + B(UBsite~UB)	kf
Proteolytic cleavages (CUT)	A + B(Domain~U) −> A + B(Domain~truncated)	kf
Degradations (DEG)	A + B −> A	kf

The table displays how the different elemental reactions in Table I are translated to the rule-based format. See Supplementary information for additional details.

figures show that the number of characterised phosphorylation reactions vastly outnumbers that of characterised dephosphorylation reactions (68 to 16; Figure 2A), and that several well-established processes are only supported by genetic data (including the entire MAP kinase cascade below Pkc1; Figure 2B, dashed lines). The reaction graph also allows comparison between the established pathway architecture and the unbiased global protein – protein interaction studies and synthetic lethal networks (Figure 3A and B, respectively).

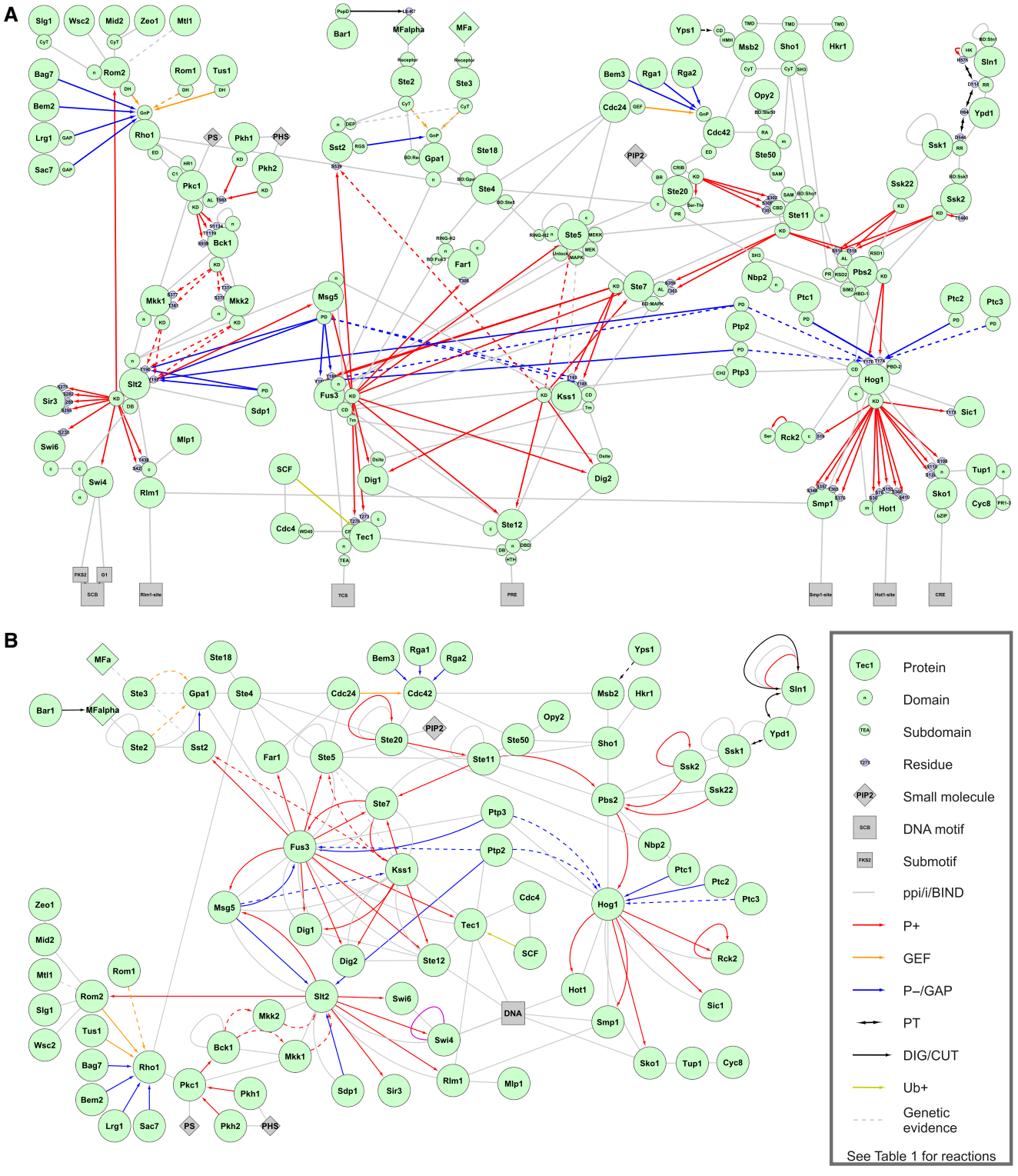

In the *contingency matrix* (Figure 4), we visualise the combined knowledge we have about the MAP kinase system (C1 and C2). The core matrix (red block of rows and blue block of columns) describe all the elemental reactions, elemental states and the (possible) contingencies of reaction on states. The black fields here show when there is no overlap between the components in the reactions and those defined in the states. Therefore, the matrix will always be sparsely populated. However, we also see that most of the remaining fields are grey; that is, effect not known ('?'). This means that our knowledge of reactions (C1; which defines rows and columns) is much stronger than our knowledge of the causality between these reactions (C2; the cells). We only have data on a minority of all possible contingencies, and these gaps are explicitly shown in the contingency matrix. It should also be noted that not all effects can be ascribed to single elemental states. We have added an outer layer of Boolean states (purple rows and columns) to account for these cases. The Boolean states describe complex mechanisms such as scaffolding and can in principle correspond to the specific states of, for example, process descriptions. However, they are only added when needed to describe empirical results. Note that only a small fraction of the states are Boolean, which reflects the low abundance of empirical data on the combinatorial effect of elemental states (i.e., specific states). Therefore, we believe it to be better to use mapping strategies which do not require such data. Finally, the matrix contains a layer of inputs and outputs (grey; columns and rows, respectively). These constitute the system's interface with the outside.

The *regulatory graph* (Figure 5) displays the information in the contingency matrix graphically, by showing how reactions produce or consume states, and how states influence reactions. This graph contains the full C1 and C2 information, and would fall apart without either. In fact, the isolated reaction–state pairs that fall outside the graph do so because they have no known incoming or outgoing contingencies. The graph shows that the MAP kinase network is rather well connected, as most reactions are indeed linked in a single graph by contingencies. However, there are relatively few input and output points; many reactions do not have known regulators and many states do not have defined regulatory effects. Only reaction–state pairs that appear between the system's input and output would be able to transmit information. This means either that all other pairs are irrelevant for the dynamics of the signal-transduction process, or that we are lacking information about their role in this process. In fact, such lose ends might be excellent candidates for targeted empirical analysis. One example would be Msb2's binding to Cdc42, which is reported to be important for the pseudohyphal differentiation pathway; raising the question of whether this binding is regulated in response to the stimuli that activate this part of the MAP kinase network. Another point that stands out is the almost complete lack of (documented) information exchange between pathways. The exception is the Sho branch of the Hog pathway, which is closely intertwined with the mating pathway, as both are activated by the shared MAP kinase kinase kinase Ste11 and parts of the cell polarity machinery.

We have also generated a network map in the established *process description* format, but without complex formations (Figure 6). This decision eliminated most of the combinatorial explosion and the need for implicit assumptions. However, there is still uncertainty in the specific phosphorylation state of the active state of certain catalysts, such as Ssk2, Ste11 and Ste7. Likewise, we do not know if phosphorylation order is an issue for proteins with multiple phosphorylation sites. In contrast to the regulatory graph (Figure 5), the process description becomes more complicated the more unknowns we have and Figure 6 is simplified (compare Supplementary Figure S2). However, the limited process description in Figure 6 clearly shows the catalyst–target relationships, and reinforces the impression that very few of the known phosphorylation reactions are balanced by known dephosphorylation reactions.

Finally, we automatically generated a mathematical description of the entire network as a proof of principle. The *rxncon* software used the contingency matrix to generate the input file for BioNetGen (Blinov *et al*, 2004). The corresponding network is too large to create but could be simulated with the network-free simulator NFSim (Sneddon *et al*, 2011). Further analysis of this system falls outside the scope of this paper, but the input file to BioNetGen and/or NFSim with trivial parameters is included as a supplement. Hence, a complete mathematical model can be automatically generated from the reaction and contingency data, and to our knowledge this is the first framework that integrates network definition at the granularity of empirical data with automatic visualisation and automatic model creation.

Discussion

It is clear that the complexity of signal-transduction networks is one of the major challenges in systems biology, impeding our ability to visualise, simulate and ultimately understand these networks. This issue has been widely recognised and substantial efforts have been committed to improve and standardise our tools for visualisation and modelling of

Figure 2 The reaction graph compactly displays the topology of the *S. cerevisiae* MAP kinase network. (**A**) The reaction graph of the MAPK network displays the components as nodes and the reactions as edges. Each component is defined by a central major node and peripheral minor nodes indicating domains, subdomains and specific residues (blue). When interacting domains and target residues are known, reactions are displayed as edges between these minor nodes. In contrast, the condensed reaction graph (**B**) displays each component as a single node, and each type of reaction between two nodes as a single edge. Nodes are either proteins (circles), small molecules (diamonds) or DNA (square). Edge colours indicate reaction type (co-substrates and co-products): Grey; protein–protein interaction (N/A), red; phosphorylation ($-$ ATP, $+$ ADP), orange; guanine nucleotide exchange ($-$ GTP, $+$ GDP), blue; dephosphorylation or GTPase activation ($+ P_i$), gold; ubiquitination ($-$ ubiquitin, $-$ ATP, $+$ ADP, $+ P_i$), black; phosphotransfer or proteolytic cleavage (N/A). The domain layout in (A) prioritises readability and domain organisation does not reflect linear sequence or protein structure. Arrowheads indicate directionality for unidirectional or reciprocal catalytic modifications. Reactions for which we found no direct evidence but which are supported by convincing genetic data has been included as dashed lines. Note the much higher frequency of reported phosphorylation reactions as compared with dephosphorylation reactions; in total the network includes 68 phosphorylation reactions but only 16 dephosphorylation reactions (A).

cellular networks (Hucka *et al*, 2003; Le Novere *et al*, 2009). These standardisation efforts are essential for data exchange and reusability, but many of the existing tools are unsuitable for definition, visualisation and mathematical modelling of large networks. The arguably most important problems are the combinatorial complexity, the granularity difference between

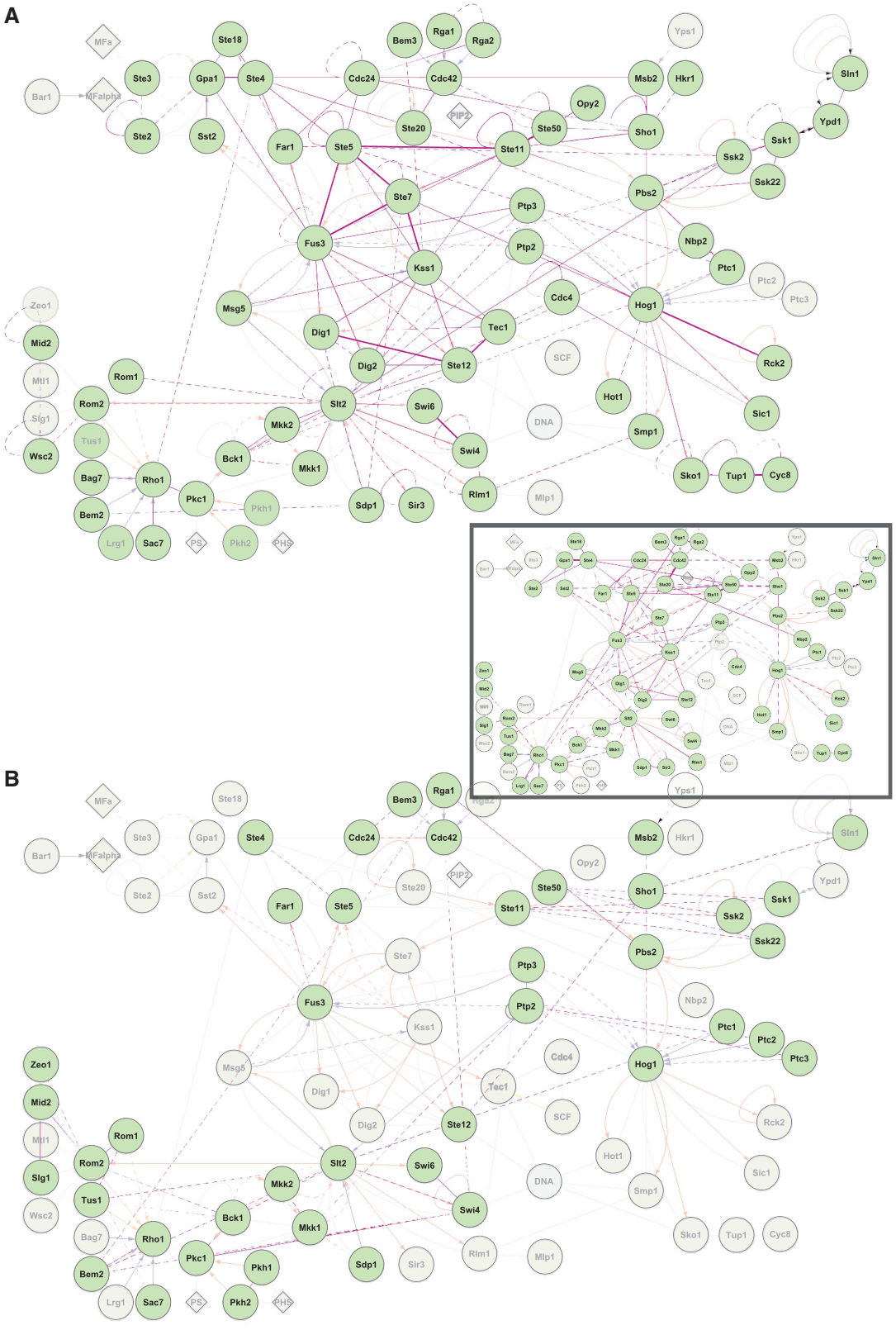

empirical and theoretical data, and the lack of exchange formats between different theoretical descriptions. Here, we have introduced a new framework for network definition at the same granularity as most empirical data. This format was already available for C1 (reaction) information, as our list of elemental reactions uses the same format as high-throughput data (PSICQUIC). We describe contextual information at the same granularity in our contingency list (C2), which not only allows an intuitive and accurate translation of empirical data but also largely avoids the combinatorial complexity. Contrary to state transition based descriptions but like the related rule-based format, the reaction and contingency based description becomes smaller the less knowledge we have as only known reactions and contingencies are considered. This format also provides for highly detailed referencing as each elemental reaction and contingency can and should be tied to empirical evidence (i.e., research paper(s)). Furthermore, we show that this format is stringent and unambiguously define both rule-based models and graphical formats, such as the activity flow diagram (condensed reaction graph), entity relationship diagram and process description formats of SBGN. Our framework also supports two new visualisation formats that we introduce here and that can display our complete knowledge database (the complete reaction and contingency lists). Finally, our framework provides a very high reusability and extendibility, as the underlying network definition—in list format—is very easy to extend, merge and reuse in other context, which is not the case for most graphically or mathematically defined systems. Of course, this level of definition still leaves the issues of parameter estimation and graphical layout, but these would typically need to be repeated even when merging graphical and mathematical network definitions. Hence, we advocate a more fundamental level of network definition than graphical or mathematical formalism. We envisage this or a similar framework as a standard to greatly facilitate model/network construction, exchange and reusability.

We have applied this method to map out the MAP kinase network of *S. cerevisiae*. This network was chosen as a benchmark since it is both well characterised and representative for signal transduction in general. It consists of three clear subgraphs, which have traditionally been considered more or less insulated pathways; the High Osmolarity Glycerol (Hog) pathway, the Protein Kinase C (PKC) pathway and the MATing (MAT) pathway, which almost completely overlaps with the PseudoHyphal Differentiation (PHD) pathway. These pathways have also been mapped or documented in several other efforts. KEGG presents a combined map of the traditional MAP kinase pathways in a format similar to its metabolic pathways (Kanehisa *et al*, 2006, 2010). However, the stringent edge definitions used for the metabolic networks have been abandoned and this is a 'biologist's graph'. The picture is similar with the maps of yeast MAP kinase pathways at Science STKE (e.g., Thorner *et al*, 2005). For example, these maps display Ste11 with four upstream regulators, but it is unclear how they regulate Ste11 and how their contributions combine (e.g., AND or OR?). Therefore, these network maps may provide an excellent introduction to the networks by providing a components list and a rough idea of the components' roles in the network, but they neither define reactions (C1) nor contingencies (C2) unambiguously. On the opposite end, we have the recently published process description of the cell cycle and its surrounding signalling network (Kaizu *et al*, 2010). This contains explicit definition of both C1 and C2 information. However, the tremendous number of specific states in such a network forces simplifications, which not only leads to a loss of knowledge, but also mixes up known contingencies (C2) with arbitrary assumptions made to simplify the network. One example in this particular case would be the separation of the upstream activation of Ste11 and its downstream effect on the Hog and Mating pathways. The output of this module is defined by the context of its activation, and this information is lost due to these arguably necessary simplifications. In addition, the granularity difference between the highly specific map states and the underlying biological data makes the mapping ambiguous, leading to further unsupported assumptions. Despite these shortcomings, the process description is useful for visualisation of certain network properties due to the explicit representation of highly detailed knowledge such as target residues. However, we stress that neither of these established and widely used methods are sufficient to accurately capture the entire signal-transduction network. Instead, we introduce the contingency matrix and the bipartite regulatory graph as alternative methods, which are able to fully capture the entire knowledge database without simplifications or assumptions. Together with the established methods, these visualisations provide an unprecedented view on the chosen benchmark system, and we trust that this completely referenced and comprehensive map of the MAP kinase signalling network in *S. cerevisiae* will be a useful reference material for the research community.

These results have direct bearing on the many efforts to create large data repositories. Pure reaction (C1) data, such as protein – protein interaction networks, can be retrieved using the standardised Molecular Interaction Query Language (MIQL; which our reaction list is designed to be compatible with) and PSICQUIC (PSICQUIC). PSICQUIC accesses, for example, ChEMBL (Overington, 2009), BioGrid (Breitkreutz *et al*, 2010), IntAct (Aranda *et al*, 2010), DIP (Xenarios *et al*, 2002), MatrixDB (Chautard *et al*, 2009) and Reactome (Croft *et al*, 2010). Several of these databases have additional information including contingency (C2) information and a standardised (non-graphical) format for definition and

Figure 3 The condensed reaction graph is an excellent tool for visualisation of high-throughput data. (**A**) Physical interactions within the MAPK network. The global protein–protein interaction network was retrieved from Biogrid (Stark *et al*, 2006), filtered for physical interactions excluding two hybrid, and visualised on the condensed reaction graph (Figure 2A). Purple edges indicate protein–protein interactions and their thickness indicates the number of times they were picked up, ranging from a single time (dashed line) to 19 times. Nodes that appear faded have no interactions with any other component in the MAPK network reported in this data set. Note that the nodes that do not correspond to single ORFs would be excluded automatically (e.g., the SCF complex, DNA, lipids). The smaller, boxed network display the corresponding two-hybrid interaction network. (**B**) Genetic interactions within the MAPK network. Synthetic lethal interactions were retrieved from Biogrid and visualised as per (A). Also quantitative data, such as mutant phenotypes and gene expression levels, can be directly visualised on the network.

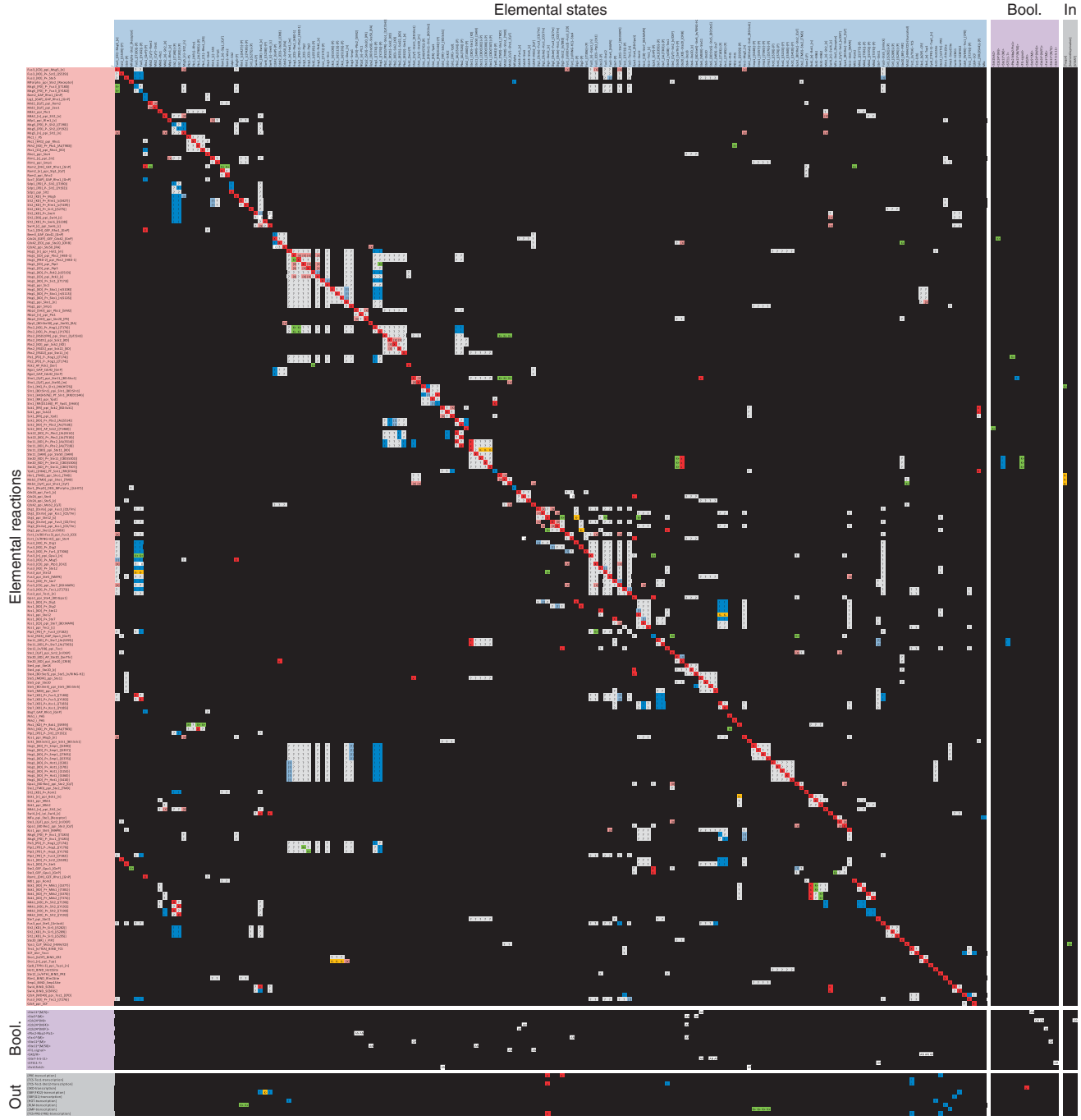

Figure 4 The contingency matrix provides a complete description of the network or network module. The core contingency matrix is spanned by the elemental reactions (rows, in red) and the elemental states (columns, in blue). The additional blocks are derived from the contingency list and contain the formation rules (rows) and effects (columns) of Boolean states (both purple) as well as the output of (rows) and input to (columns) the network (both grey). The cells in the matrix define how each reaction (row) depends on each state (column). The effects range from being absolutely required ('!'), via positive effector ('K +'), no effect ('0') and negative effector ('K–') to absolutely inhibitory ('x'), or it can be unknown or undefined ('?'). Each Boolean state is defined by a single operator ('AND' or 'OR') for the elemental states, other Booleans and/or inputs that defines it. The contingency matrix displayed here contains the complete MAPK network. Note that the contingency matrix is sparsely populated. This is both because most combinations of reactions and states lack overlap in components (black squares) and because we have very limited knowledge of the possible contingencies (grey squares). Overall, the information on what reactions can occur is much more abundant than on how they are regulated.

retrieval would further improve the usefulness of these resources and facilitate further analysis of the stored information. The framework we propose here provides such a format with the key advantage of including export to mathematical models. Since mathematical modelling is the most central and natural step to bring the knowledge in these databases into a useful form, where quantitative systems properties can most exhaustively be analysed, the introduction of such an export is

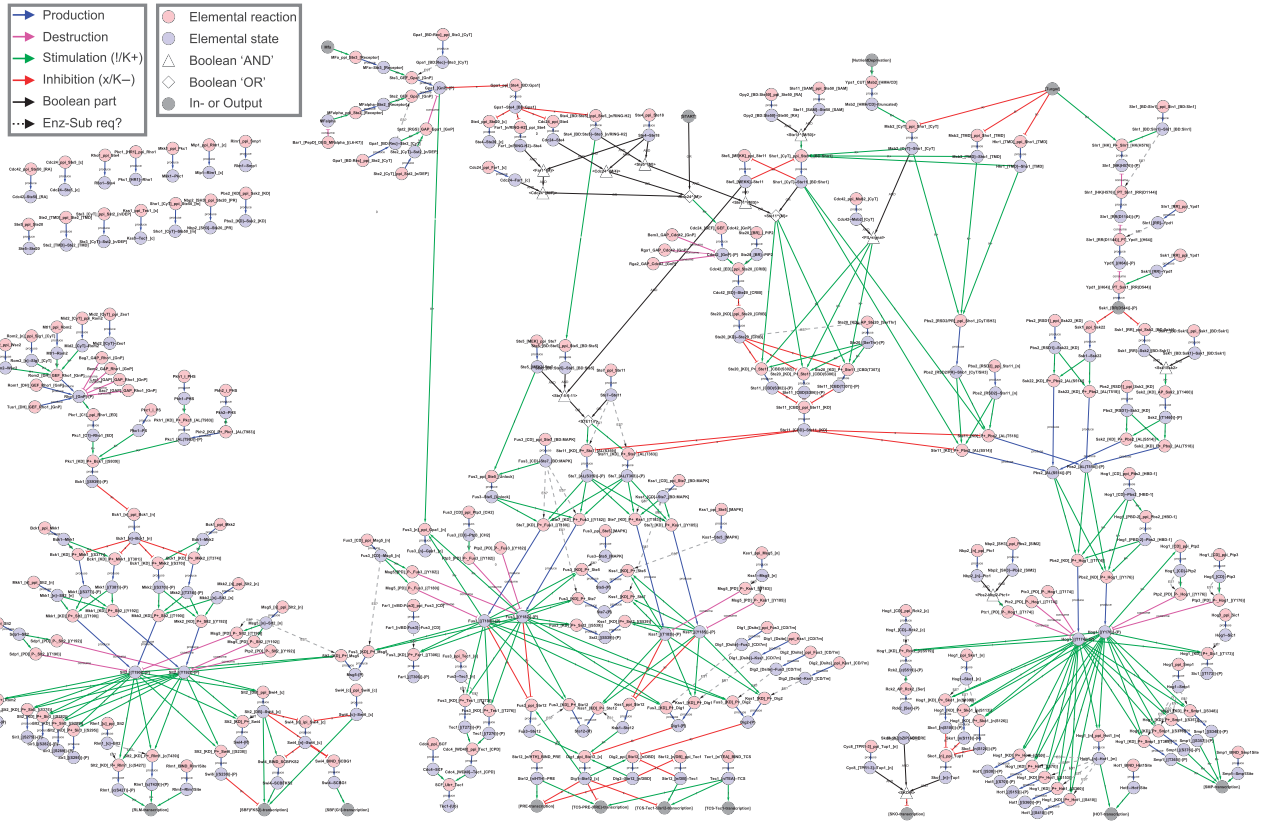

Figure 5 The regulatory graph visualise the causality between reactions and reveals the regulatory structure of the network. This bipartite graph illustrates the relationships between the reactions (red nodes) and states (blue nodes) within the network. Edges from reactions to states define how states are produced (blue) or consumed (purple), and each such edge corresponds to a single elemental reaction. Edges from states to reactions define how states regulate other reactions, and each such edge correspond to a single contingency (Green; absolute requirement ('!') or positive effector ('K +'), red; negative effector ('K–') or absolutely inhibitory ('x')). Booleans are used when the effect on a reaction cannot be attributed to single elemental states (white diamonds (OR) or triangles (AND) connected to the states/Booleans/inputs that define them with black lines). Inputs are displayed in grey and connected to the elemental reaction(s) they influence. Likewise, outputs are displayed in grey and connected to the states they are influenced by. Signals can be followed through the network from external cues (grey; top) to transcriptional response (grey; bottom) as all edges are directional. Reactions without input are not (known to be) regulated and would therefore be expected to have constant rates; likewise states without output have no (defined) impact on the system. We have also included likely but undocumented requirements for enzyme–substrate bindings before catalysis as dashed lines. The regulatory graph is the only graphical representation using the complete information in the contingency matrix, and hence the only complete and completely graphical visualisation of the network. It is also the most potent visualisation to evaluate the degree of knowledge about the network. For example, visualisation of high-throughput data would result in disconnected reaction–state pairs only, due to the lack of regulatory information (no C2 data).

an important step forward. This framework is still not as flexible as direct model definition but it provides distinct advantages. Formulating models directly using classical state transition reactions is either subjective or very cumbersome in practice due to the combinatorial explosion, and state transition based models for the networks of the size we consider here are too large to be simulated. The closest related modelling framework is rule-based modelling, in which models can be formulated without these combinatorial explosion problems, and it is also to a rule-based format that we export our models. However, the classical rule-based modelling frameworks lack all the database properties of our framework, such as the contingency matrix and its export to various novel visualisation formats. In short, one could therefore say that our framework combines the best of existing knowledge databases with new visualisation tools and rule-based modelling.

In conclusion, we present a method to document and visualise signal-transduction networks that improves on previous strategies in the following respects; (I) it allows concise mapping at the same granularity as biological data, hence pre-empting the need for implicit, unsupported assumptions, (II) it allows referencing of each elemental reaction and contingency separately and handles unknowns explicitly, (III) the network can be visualised without any simplifications or assumptions that increase the uncertainty, (IV) the visualisations can be automatically generated from the data files, (V) the network definition is a template from which a mathematical model can be automatically generated (VI) and exported to SBML and (VII) the supplied template and *rxncon* tool makes the method immediately useful for anyone with an interest in signal transduction. Hence, our framework bridge three critical levels of signal-transduction network analysis; definition, visualisation and mathematical modelling, as well as empirical data and theoretical analysis.

Materials and methods

The MAP kinase network map is based on the papers listed below. The specific reference(s) are listed for each reaction and contingency

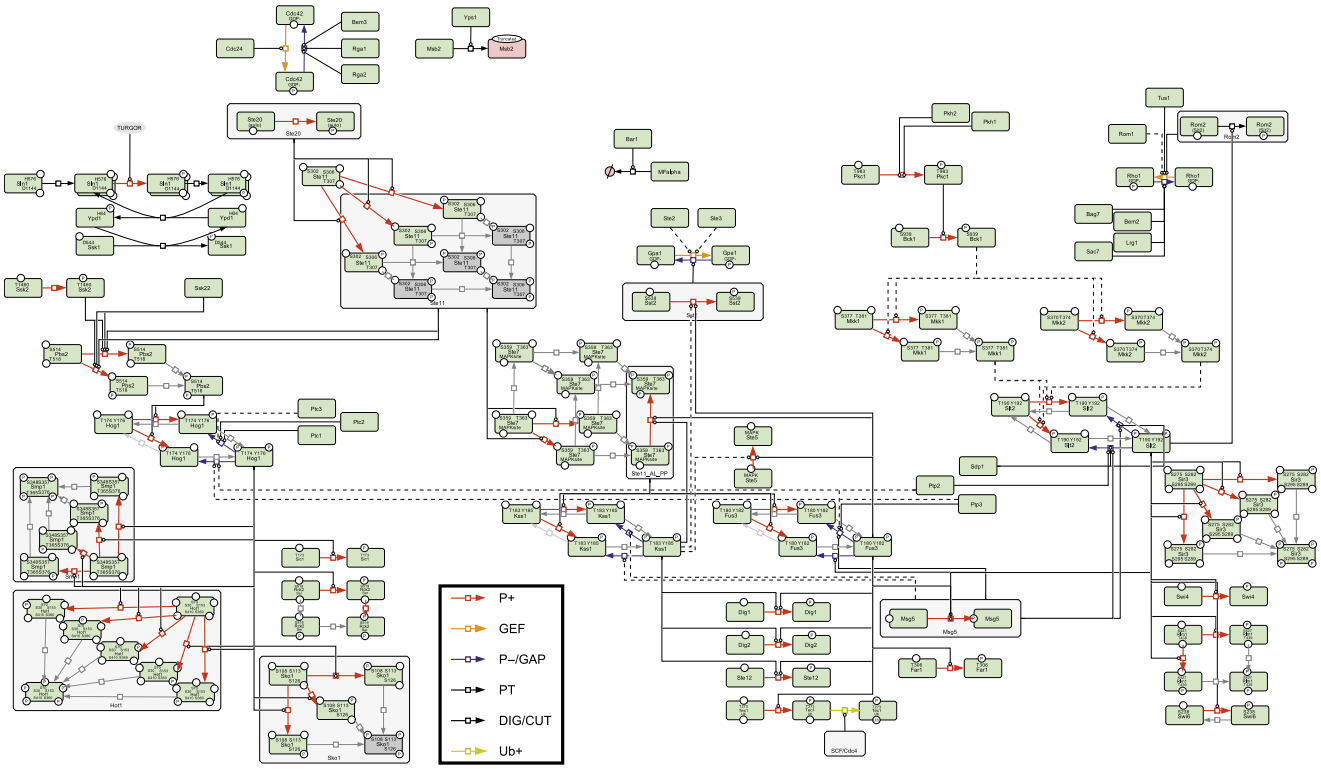

Figure 6 The limited process description displays all posttranslational modifications and their catalysts, but excludes complex formation. Each specific internal state is represented as a distinct node, although some intermediate phosphorylation states have been excluded. Phosphorylations are indicated with red arrows (ATP as co-substrate and ADP as co-product), GEF reactions as orange arrows (− GTP, + GDP), and dephosphorylation or GAP reactions as blue arrows (+ P_i). Only a fraction of the catalytic modifications have a known catalyst for both forward and reverse reactions, and the required state of the catalyst known is in even fewer cases. Therefore, even this highly simplified process description includes uncertainty in the required states of both catalysts and substrates. In this visualisation, this uncertainty has been shown by using a single catalysis arrow from a box including all potentially active state of the catalyst to the basic state of the substrate (completely unphosphorylated for kinase reactions, or completely phosphorylated for phosphatase reactions). While these simplifications are unsupported, including additional catalytic arrows would be equally arbitrary with the added drawback of making the figure more complex (see Supplementary Figure S2). Despite the need for implicit assumptions, the process description is useful as it is very explicit and intuitive to read.

individually in the reaction and contingency lists in the 'PubMedIdentifier(s)' column with their PMID number.

(Ai *et al*, 2002; Alepuz *et al*, 2003; Alepuz *et al*, 2001; Andrews and Herskowitz, 1989; Andrews and Moore, 1992; Apanovitch *et al*, 1998; Baetz and Andrews, 1999; Baetz *et al*, 2001; Ballon *et al*, 2006; Bao *et al*, 2004; Bao *et al*, 2010; Bar *et al*, 2003; Bardwell *et al*, 1996; Bardwell *et al*, 1998a; Bardwell *et al*, 1998b; Bender and Sprague, 1986; Bilsland-Marchesan *et al*, 2000; Blumer *et al*, 1988; Breitkreutz *et al*, 2001; Bruckner *et al*, 2004; Butty *et al*, 1998; Chou *et al*, 2004; Chou *et al*, 2006; Cismowski *et al*, 2001; Clark *et al*, 1993; Collister *et al*, 2002; Cook *et al*, 1996; Crosby *et al*, 2000; Cullen *et al*, 2004; Davenport *et al*, 1999; de Nadal *et al*, 2003; Dodou and Treisman, 1997; Doi *et al*, 1994; Dolan *et al*, 1989; Dowell *et al*, 1998; Drogen *et al*, 2000; Elion *et al*, 1993; Errede *et al*, 1993; Escote *et al*, 2004; Feng *et al*, 1998; Fitch *et al*, 2004; Flandez *et al*, 2004; Flotho *et al*, 2004; Friant *et al*, 2001; Garcia-Gimeno and Struhl, 2000; Garrison *et al*, 1999; Gartner *et al*, 1998; Gartner *et al*, 1992; Good *et al*, 2009; Green *et al*, 2003; Guo *et al*, 2009; Hagen *et al*, 1986; Hagen *et al*, 1991; Hahn and Thiele, 2002; Heenan *et al*, 2009; Heise *et al*, 2010; Ho *et al*, 2002; Horie *et al*, 2008; Inagaki *et al*, 1999; Inouye *et al*, 1997a; Inouye *et al*, 1997b; Irie *et al*, 1993; Jacoby *et al*, 1997; Jung *et al*, 2002; Kamada *et al*, 1995; Kamada *et al*, 1996; Ketela *et al*, 1999; Kim *et al*, 2010; Kim *et al*, 2008; Kranz *et al*, 1994; Kusari *et al*, 2004; Lamson *et al*, 2002; Lee and Levin, 1992; Leeuw *et al*, 1995; Leeuw *et al*, 1998; Li *et al*, 1998; Liu *et al*, 2005; MacKay *et al*, 1991; MacKay *et al*, 1988; Madden *et al*, 1997; Madhani and Fink, 1997; Madhani *et al*, 1997; Maeda *et al*, 1995; Maeda *et al*, 1994; Maleri *et al*, 2004; Mapes and Ota, 2004; Martin *et al*, 2000; Mattison and Ota, 2000; Mattison *et al*, 1999; Medici *et al*, 1997; Melcher and Thorner, 1996; Metodiev *et al*, 2002; Miyajima *et al*, 1987; Murakami *et al*, 2008; Nasmyth and Dirick, 1991; Nehlin *et al*, 1992; Neiman and Herskowitz, 1994; Nern and Arkowitz, 1998; Nern and Arkowitz, 1999; Nonaka *et al*, 1995; Olson *et al*, 2000; Ostrander and Gorman, 1999; Ozaki *et al*, 1996; Paravicini and Friedli, 1996; Parnell *et al*, 2005; Pascual-Ahuir *et al*, 2001; Peter *et al*, 1996; Peterson *et al*, 1994; Philip and Levin, 2001; Posas and Saito, 1997; Posas and Saito, 1998; Posas *et al*, 1998; Posas *et al*, 1996; Proft *et al*, 2005; Proft *et al*, 2001; Proft and Serrano, 1999; Proft and Struhl, 2002; Raicu *et al*, 2005; Raitt *et al*, 2000; Rajavel *et al*, 1999; Reiser *et al*, 2000; Remenyi *et al*, 2005; Rep *et al*, 2000; Rep *et al*, 1999; Roberts and Fink, 1994; Schmelzle *et al*, 2002; Schmidt *et al*, 1997; Schmidt *et al*, 2002; Schmitz *et al*, 2002; Shi *et al*, 2005; Shimada *et al*, 2004; Sidorova and Breeden, 1993; Siegmund and Nasmyth, 1996; Siekhaus and Drubin, 2003; Simon *et al*, 1995; Skowyra *et al*, 1997; Smith *et al*, 2002; Soler *et al*, 1995; Song *et al*, 1996; Taba *et al*, 1991; Takahashi and Pryciak, 2007; Tao *et al*, 2002; Tarassov *et al*, 2008; Tatebayashi *et al*, 2003; Tatebayashi *et al*, 2007; Tatebayashi *et al*, 2006; Tedford *et al*, 1997; Truckses *et al*, 2006; Truman *et al*, 2009; Vadaie *et al*, 2008; Valtz *et al*, 1995; Varanasi *et al*, 1996; Verna *et al*, 1997; Vilella *et al*, 2005; Wang and Konopka, 2009; Wang *et al*, 2005; Warmka *et al*, 2001; Wassmann and Ammerer, 1997; Watanabe *et al*, 1994; Watanabe *et al*, 1995; Watanabe *et al*, 1997; Winters and Pryciak, 2005; Wu *et al*, 2006; Wu *et al*, 1999; Wu *et al*, 1995; Wu *et al*, 2004; Wurgler-Murphy *et al*, 1997; Yablonski *et al*, 1996; Yamamoto *et al*, 2010; Yesilaltay and Jenness, 2000; Young *et al*, 2002; Yuan and Fields, 1991; Zarrinpar *et al*, 2004;

Zarrinpar *et al*, 2003; Zarzov *et al*, 1996; Zeitlinger *et al*, 2003; Zhan *et al*, 1997; Zhan and Guan, 1999; Zhao *et al*, 1995; Zheng and Guan, 1994; Zheng *et al*, 1994; Zhou *et al*, 1993).

The methods used are an integral part of the results and are outlined in that section. For additional details, please see Supplementary information.

Supplementary information

Supplementary information is available at the *Molecular Systems Biology* website (www.nature.com/msb).

Conflict of interest

The authors declare that they have no conflict of interest.

Acknowledgements

We thank past and present colleagues for helpful discussions; in particular Akira Funahashi, Noriko Hiroi and Douglas Murray for suggestions in the conception phase, Hans-Michael Kaltenbach for introduction to the bipartite graph, Clemens Kühn for introduction to NFsim, Jens Nielsen for the suggestion to use matrix multiplication to calculate network distance and Nina Arens for proofreading. We acknowledge support from JSPS and SSF (Japan-Sweden collaborative postdoc grant to MK), Lions and the Swedish Research Council (to GC), the German Ministry for Education and Research (BMBF, SysMO2 project Translucent 2 to EK), the European Commission (UNICELLSYS, Grant 201142, AQUAGLYCEROPORIN, Grant 35995, CELLCOMPUT, Grant 043310 and SYSTEMSBIOLOGY, Grant 514169, all to SH and EK) and from the MULTIDISCIPLINARY BIO Sweden-Japan initiative (Sweden: Foundation for Strategic Research SSF and Vinnova, Japan: Japan Science and Technology Agency JST) to SH and HK. Work in the laboratory of SH was also supported by a grant from the Swedish Research Council (Grant 2007-4905).

Author contributions: HK initiated the mapping project. MK conceived the framework. GC and MK developed the framework with input from all the authors. CFT and MK mapped the MAP kinase network. FK and RP implemented the framework with guidance from GC and MK. FK created the *rxncon* software tool. MK drafted the first manuscript with help from GC. SH and EK contributed biological and theoretical background knowledge, respectively. SH, EK and HK provided the research environments and contributed to completion of the manuscript. All authors read, edited and approved the final manuscript.

References

Ai W, Bertram PG, Tsang CK, Chan TF, Zheng XF (2002) Regulation of subtelomeric silencing during stress response. *Mol Cell* **10:** 1295–1305

Alepuz PM, de Nadal E, Zapater M, Ammerer G, Posas F (2003) Osmostress-induced transcription by Hot1 depends on a Hog1-mediated recruitment of the RNA Pol II. *EMBO J* **22:** 2433–2442

Alepuz PM, Jovanovic A, Reiser V, Ammerer G (2001) Stress-induced map kinase Hog1 is part of transcription activation complexes. *Mol Cell* **7:** 767–777

Andrews BJ, Herskowitz I (1989) Identification of a DNA binding factor involved in cell-cycle control of the yeast HO gene. *Cell* **57:** 21–29

Andrews BJ, Moore LA (1992) Interaction of the yeast Swi4 and Swi6 cell cycle regulatory proteins in vitro. *Proc Natl Acad Sci USA* **89:** 11852–11856

Apanovitch DM, Slep KC, Sigler PB, Dohlman HG (1998) Sst2 is a GTPase-activating protein for Gpa1: purification and characterization of a cognate RGS-Galpha protein pair in yeast. *Biochemistry* **37:** 4815–4822

Aranda B, Achuthan P, Alam-Faruque Y, Armean I, Bridge A, Derow C, Feuermann M, Ghanbarian AT, Kerrien S, Khadake J, Kerssemakers J, Leroy C, Menden M, Michaut M, Montecchi-Palazzi L, Neuhauser SN, Orchard S, Perreau V, Roechert B, van Eijk K *et al* (2010) The IntAct molecular interaction database in 2010. *Nucleic Acids Res* **38:** D525–D531

Baetz K, Andrews B (1999) Regulation of cell cycle transcription factor Swi4 through auto-inhibition of DNA binding. *Mol Cell Biol* **19:** 6729–6741

Baetz K, Moffat J, Haynes J, Chang M, Andrews B (2001) Transcriptional coregulation by the cell integrity mitogen-activated protein kinase Slt2 and the cell cycle regulator Swi4. *Mol Cell Biol* **21:** 6515–6528

Ballon DR, Flanary PL, Gladue DP, Konopka JB, Dohlman HG, Thorner J (2006) DEP-domain-mediated regulation of GPCR signaling responses. *Cell* **126:** 1079–1093

Bao MZ, Schwartz MA, Cantin GT, Yates JR3rd, Madhani HD (2004) Pheromone-dependent destruction of the Tec1 transcription factor is required for MAP kinase signaling specificity in yeast. *Cell* **119:** 991–1000

Bao MZ, Shock TR, Madhani HD (2010) Multisite phosphorylation of the Saccharomyces cerevisiae filamentous growth regulator Tec1 is required for its recognition by the E3 ubiquitin ligase adaptor Cdc4 and its subsequent destruction in vivo. *Eukaryot Cell* **9:** 31–36

Bar EE, Ellicott AT, Stone DE (2003) Gbetagamma recruits Rho1 to the site of polarized growth during mating in budding yeast. *J Biol Chem* **278:** 21798–21804

Bardwell L, Cook JG, Chang EC, Cairns BR, Thorner J (1996) Signaling in the yeast pheromone response pathway: specific and high-affinity interaction of the mitogen-activated protein (MAP) kinases Kss1 and Fus3 with the upstream MAP kinase kinase Ste7. *Mol Cell Biol* **16:** 3637–3650

Bardwell L, Cook JG, Voora D, Baggott DM, Martinez AR, Thorner J (1998a) Repression of yeast Ste12 transcription factor by direct binding of unphosphorylated Kss1 MAPK and its regulation by the Ste7 MEK. *Genes Dev* **12:** 2887–2898

Bardwell L, Cook JG, Zhu-Shimoni JX, Voora D, Thorner J (1998b) Differential regulation of transcription: repression by unactivated mitogen-activated protein kinase Kss1 requires the Dig1 and Dig2 proteins. *Proc Natl Acad Sci USA* **95:** 15400–15405

Bender A, Sprague GFJr. (1986) Yeast peptide pheromones, a-factor and alpha-factor, activate a common response mechanism in their target cells. *Cell* **47:** 929–937

Bilsland-Marchesan E, Arino J, Saito H, Sunnerhagen P, Posas F (2000) Rck2 kinase is a substrate for the osmotic stress-activated mitogen-activated protein kinase Hog1. *Mol Cell Biol* **20:** 3887–3895

Biographer http://code.google.com/p/biographer/

Blinov ML, Faeder JR, Goldstein B, Hlavacek WS (2004) BioNetGen: software for rule-based modeling of signal transduction based on the interactions of molecular domains. *Bioinformatics (Oxford, England)* **20:** 3289–3291

Blinov ML, Yang J, Faeder JR, Hlavacek WS (2006) Depicting signaling cascades. *Nature Biotechnology* **24:** 137–138author reply 138

Blumer KJ, Reneke JE, Thorner J (1988) The STE2 gene product is the ligand-binding component of the alpha-factor receptor of Saccharomyces cerevisiae. *J Biol Chem* **263:** 10836–10842

Borisov NM, Chistopolsky AS, Faeder JR, Kholodenko BN (2008) Domain-oriented reduction of rule-based network models. *IET Syst Biol* **2:** 342–351

Breitkreutz A, Boucher L, Tyers M (2001) MAPK specificity in the yeast pheromone response independent of transcriptional activation. *Curr Biol* **11:** 1266–1271

Breitkreutz A, Choi H, Sharom JR, Boucher L, Neduva V, Larsen B, Lin ZY, Breitkreutz BJ, Stark C, Liu G, Ahn J, Dewar-Darch D, Reguly T, Tang X, Almeida R, Qin ZS, Pawson T, Gingras AC, Nesvizhskii AI, Tyers M (2010) A global protein kinase and phosphatase interaction network in yeast. *Science (New York, NY)* **328:** 1043–1046

Bruckner S, Kohler T, Braus GH, Heise B, Bolte M, Mosch HU (2004) Differential regulation of Tec1 by Fus3 and Kss1 confers signaling specificity in yeast development. *Curr Genet* **46:** 331–342

Butty AC, Pryciak PM, Huang LS, Herskowitz I, Peter M (1998) The role of Far1p in linking the heterotrimeric G protein to polarity establishment proteins during yeast mating. *Science* **282:** 1511–1516

Chautard E, Ballut L, Thierry-Mieg N, Ricard-Blum S (2009) MatrixDB, a database focused on extracellular protein-protein and protein-carbohydrate interactions. *Bioinformatics (Oxford, England)* **25:** 690–691

Chou S, Huang L, Liu H (2004) Fus3-regulated Tec1 degradation through SCFCdc4 determines MAPK signaling specificity during mating in yeast. *Cell* **119:** 981–990

Chou S, Lane S, Liu H (2006) Regulation of mating and filamentation genes by two distinct Ste12 complexes in Saccharomyces cerevisiae. *Mol Cell Biol* **26:** 4794–4805

Chylek LA, Hu B, Blinov ML, Emonet T, Faeder JR, Goldstein B, Gutenkunst RN, Haugh JM, Lipniacki T, Posner RG, Yang J, Hlavacek WS (2011) Guidelines for visualizing and annotating rule-based models. *Mol Biol Syst* **7:** 2779–2795

Cismowski MJ, Metodiev M, Draper E, Stone DE (2001) Biochemical analysis of yeast G(alpha) mutants that enhance adaptation to pheromone. *Biochem Biophys Res Commun* **284:** 247–254

Clark KL, Dignard D, Thomas DY, Whiteway M (1993) Interactions among the subunits of the G protein involved in Saccharomyces cerevisiae mating. *Mol Cell Biol* **13:** 1–8

Collister M, Didmon MP, MacIsaac F, Stark MJ, MacDonald NQ, Keyse SM (2002) YIL113w encodes a functional dual-specificity protein phosphatase which specifically interacts with and inactivates the Slt2/Mpk1p MAP kinase in S. cerevisiae. *FEBS Lett* **527:** 186–192

Conzelmann H, Fey D, Gilles ED (2008) Exact model reduction of combinatorial reaction networks. *BMC Syst Biol* **2:** 78

Cook JG, Bardwell L, Kron SJ, Thorner J (1996) Two novel targets of the MAP kinase Kss1 are negative regulators of invasive growth in the yeast Saccharomyces cerevisiae. *Genes Dev* **10:** 2831–2848

Croft D, O'Kelly G, Wu G, Haw R, Gillespie M, Matthews L, Caudy M, Garapati P, Gopinath G, Jassal B, Jupe S, Kataskaya I, Mahajan S, May B, Ndegwa N, Schmidt E, Shamovsky V, Yung C, Birney E, Hermjakob H *et al* (2010) *Reactome: a database of reactions, pathways and biological processesNucleic Acids Res* ***39****(Database issue): D691–D697*

Crosby JA, Konopka JB, Fields S (2000) Constitutive activation of the Saccharomyces cerevisiae transcriptional regulator Ste12p by mutations at the amino-terminus. *Yeast* **16:** 1365–1375

Cullen PJ, Sabbagh WJr., Graham E, Irick MM, van Olden EK, Neal C, Delrow J, Bardwell L, Sprague GFJr. (2004) A signaling mucin at the head of the Cdc42- and MAPK-dependent filamentous growth pathway in yeast. *Genes Dev* **18:** 1695–1708

Danos V (2007) Rule-based modelling of cellular signalling. *Cell Signal* 17–41

Davenport KD, Williams KE, Ullmann BD, Gustin MC (1999) Activation of the Saccharomyces cerevisiae filamentation/invasion pathway by osmotic stress in high-osmolarity glycogen pathway mutants. *Genetics* **153:** 1091–1103

de Nadal E, Casadome L, Posas F (2003) Targeting the MEF2-like transcription factor Smp1 by the stress-activated Hog1 mitogen-activated protein kinase. *Mol Cell Biol* **23:** 229–237

Dodou E, Treisman R (1997) The Saccharomyces cerevisiae MADS-box transcription factor Rlm1 is a target for the Mpk1 mitogen-activated protein kinase pathway. *Mol Cell Biol* **17:** 1848–1859

Doi K, Gartner A, Ammerer G, Errede B, Shinkawa H, Sugimoto K, Matsumoto K (1994) MSG5, a novel protein phosphatase promotes adaptation to pheromone response in S. cerevisiae. *EMBO J* **13:** 61–70

Dolan JW, Kirkman C, Fields S (1989) The yeast STE12 protein binds to the DNA sequence mediating pheromone induction. *Proc Natl Acad Sci USA* **86:** 5703–5707

Dowell SJ, Bishop AL, Dyos SL, Brown AJ, Whiteway MS (1998) Mapping of a yeast G protein betagamma signaling interaction. *Genetics* **150:** 1407–1417

Drogen F, O'Rourke SM, Stucke VM, Jaquenoud M, Neiman AM, Peter M (2000) Phosphorylation of the MEKK Ste11p by the PAK-like kinase Ste20p is required for MAP kinase signaling in vivo. *Curr Biol* **10:** 630–639

Elion EA, Satterberg B, Kranz JE (1993) FUS3 phosphorylates multiple components of the mating signal transduction cascade: evidence for STE12 and FAR1. *Mol Biol Cell* **4:** 495–510

Errede B, Gartner A, Zhou Z, Nasmyth K, Ammerer G (1993) MAP kinase-related FUS3 from S. cerevisiae is activated by STE7 in vitro. *Nature* **362:** 261–264

Escote X, Zapater M, Clotet J, Posas F (2004) Hog1 mediates cell-cycle arrest in G1 phase by the dual targeting of Sic1. *Nat Cell Biol* **6:** 997–1002

Faeder JR, Blinov ML, Goldstein B, Hlavacek WS (2005) Rule-based modeling of biochemical networks. *Complexity* **10:** 22–41

Feng Y, Song LY, Kincaid E, Mahanty SK, Elion EA (1998) Functional binding between Gbeta and the LIM domain of Ste5 is required to activate the MEKK Ste11. *Curr Biol* **8:** 267–278

Fitch PG, Gammie AE, Lee DJ, de Candal VB, Rose MD (2004) Lrg1p Is a Rho1 GTPase-activating protein required for efficient cell fusion in yeast. *Genetics* **168:** 733–746

Flandez M, Cosano IC, Nombela C, Martin H, Molina M (2004) Reciprocal regulation between Slt2 MAPK and isoforms of Msg5 dual-specificity protein phosphatase modulates the yeast cell integrity pathway. *J Biol Chem* **279:** 11027–11034

Flotho A, Simpson DM, Qi M, Elion EA (2004) Localized feedback phosphorylation of Ste5p scaffold by associated MAPK cascade *J Biol Chem* **279:** 47391–47401

Friant S, Lombardi R, Schmelzle T, Hall MN, Riezman H (2001) Sphingoid base signaling via Pkh kinases is required for endocytosis in yeast. *EMBO J* **20:** 6783–6792

Garcia-Gimeno MA, Struhl K (2000) Aca1 and Aca2, ATF/CREB activators in Saccharomyces cerevisiae, are important for carbon source utilization but not the response to stress. *Mol Cell Biol* **20:** 4340–4349

Garrison TR, Zhang Y, Pausch M, Apanovitch D, Aebersold R, Dohlman HG (1999) Feedback phosphorylation of an RGS protein by MAP kinase in yeast. *J Biol Chem* **274:** 36387–36391

Gartner A, Jovanovic A, Jeoung DI, Bourlat S, Cross FR, Ammerer G (1998) Pheromone-dependent G1 cell cycle arrest requires Far1 phosphorylation, but may not involve inhibition of Cdc28-Cln2 kinase, in vivo. *Mol Cell Biol* **18:** 3681–3691

Gartner A, Nasmyth K, Ammerer G (1992) Signal transduction in Saccharomyces cerevisiae requires tyrosine and threonine phosphorylation of FUS3 and KSS1. *Genes Dev* **6:** 1280–1292

Good M, Tang G, Singleton J, Remenyi A, Lim WA (2009) The Ste5 scaffold directs mating signaling by catalytically unlocking the Fus3 MAP kinase for activation. *Cell* **136:** 1085–1097

Green R, Lesage G, Sdicu AM, Menard P, Bussey H (2003) A synthetic analysis of the Saccharomyces cerevisiae stress sensor Mid2p, and identification of a Mid2p-interacting protein, Zeo1p, that modulates the PKC1-MPK1 cell integrity pathway. *Microbiology* **149:** 2487–2499

Guo S, Shen X, Yan G, Ma D, Bai X, Li S, Jiang Y (2009) A MAP kinase dependent feedback mechanism controls Rho1 GTPase and actin distribution in yeast. *PLoS One* **4:** e6089

Hagen DC, McCaffrey G, Sprague GFJr. (1986) Evidence the yeast STE3 gene encodes a receptor for the peptide pheromone a factor: gene sequence and implications for the structure of the presumed receptor. *Proc Natl Acad Sci USA* **83:** 1418–1422

Hagen DC, McCaffrey G, Sprague GFJr. (1991) Pheromone response elements are necessary and sufficient for basal and pheromone-induced transcription of the FUS1 gene of Saccharomyces cerevisiae. *Mol Cell Biol* **11:** 2952–2961

Hahn JS, Thiele DJ (2002) Regulation of the Saccharomyces cerevisiae Slt2 kinase pathway by the stress-inducible Sdp1 dual specificity phosphatase. *J Biol Chem* **277:** 21278–21284

Heenan EJ, Vanhooke JL, Temple BR, Betts L, Sondek JE, Dohlman HG (2009) Structure and function of Vps15 in the endosomal G protein signaling pathway. *Biochemistry* **48:** 6390–6401

Heise B, van der Felden J, Kern S, Malcher M, Bruckner S, Mosch HU (2010) The TEA transcription factor Tec1 confers promoter-specific gene regulation by Ste12-dependent and -independent mechanisms. *Eukaryot Cell* **9:** 514–531

Hlavacek WS, Faeder JR, Blinov ML, Perelson AS, Goldstein B (2003) The complexity of complexes in signal transduction. *Biotechnol Bioeng* **84:** 783–794

Ho Y, Gruhler A, Heilbut A, Bader GD, Moore L, Adams SL, Millar A, Taylor P, Bennett K, Boutilier K, Yang L, Wolting C, Donaldson I, Schandorff S, Shewnarane J, Vo M, Taggart J, Goudreault M, Muskat B, Alfarano C *et al* (2002) Systematic identification of protein complexes in Saccharomyces cerevisiae by mass spectrometry. *Nature* **415:** 180–183

Horie T, Tatebayashi K, Yamada R, Saito H (2008) Phosphorylated Ssk1 prevents unphosphorylated Ssk1 from activating the Ssk2 mitogen-activated protein kinase kinase kinase in the yeast high-osmolarity glycerol osmoregulatory pathway. *Mol Cell Biol* **28:** 5172–5183

Hucka M, Finney A, Sauro HM, Bolouri H, Doyle JC, Kitano H, Arkin AP, Bornstein BJ, Bray D, Cornish-Bowden A, Cuellar AA, Dronov S, Gilles ED, Ginkel M, Gor V, Goryanin II, Hedley WJ, Hodgman TC, Hofmeyr JH, Hunter PJ *et al* (2003) The systems biology markup language (SBML): a medium for representation and exchange of biochemical network models. *Bioinformatics (Oxford, England)* **19:** 524–531

Inagaki M, Schmelzle T, Yamaguchi K, Irie K, Hall MN, Matsumoto K (1999) PDK1 homologs activate the Pkc1-mitogen-activated protein kinase pathway in yeast. *Mol Cell Biol* **19:** 8344–8352

Inouye C, Dhillon N, Durfee T, Zambryski PC, Thorner J (1997a) Mutational analysis of STE5 in the yeast Saccharomyces cerevisiae: application of a differential interaction trap assay for examining protein-protein interactions. *Genetics* **147:** 479–492

Inouye C, Dhillon N, Thorner J (1997b) Ste5 RING-H2 domain: role in Ste4-promoted oligomerization for yeast pheromone signaling. *Science* **278:** 103–106

Irie K, Takase M, Lee KS, Levin DE, Araki H, Matsumoto K, Oshima Y (1993) MKK1 and MKK2, which encode Saccharomyces cerevisiae mitogen-activated protein kinase-kinase homologs, function in the pathway mediated by protein kinase C. *Mol Cell Biol* **13:** 3076–3083

Jacoby T, Flanagan H, Faykin A, Seto AG, Mattison C, Ota I (1997) Two protein-tyrosine phosphatases inactivate the osmotic stress response pathway in yeast by targeting the mitogen-activated protein kinase, Hog1. *J Biol Chem* **272:** 17749–17755

Jung US, Sobering AK, Romeo MJ, Levin DE (2002) Regulation of the yeast Rlm1 transcription factor by the Mpk1 cell wall integrity MAP kinase. *Mol Microbiol* **46:** 781–789

Kaizu K, Ghosh S, Matsuoka Y, Moriya H, Shimizu-Yoshida Y, Kitano H (2010) A comprehensive molecular interaction map of the budding yeast cell cycle. *Mol Syst Biol* **6:** 415

Kaltenbach H-M, Constantinescu S, Feigelman J, Stelling J (2011) *Graph-Based Decomposition of Biochemical Reaction Networks Into Monotone Subsystems Algorithms in Bioinformatics*, Przytycka T, Sagot M-F (eds) Vol. 6833, pp 139–150SpringerBerlin/Heidelberg

Kamada Y, Jung US, Piotrowski J, Levin DE (1995) The protein kinase C-activated MAP kinase pathway of Saccharomyces cerevisiae mediates a novel aspect of the heat shock response. *Genes Dev* **9:** 1559–1571

Kamada Y, Qadota H, Python CP, Anraku Y, Ohya Y, Levin DE (1996) Activation of yeast protein kinase C by Rho1 GTPase. *J Biol Chem* **271:** 9193–9196

Kanehisa M, Goto S, Furumichi M, Tanabe M, Hirakawa M (2010) KEGG for representation and analysis of molecular networks involving diseases and drugs. *Nucleic Acids Res* **38:** D355–D360

Kanehisa M, Goto S, Hattori M, Aoki-Kinoshita KF, Itoh M, Kawashima S, Katayama T, Araki M, Hirakawa M (2006) From genomics to chemical genomics: new developments in KEGG. *Nucleic Acids Res* **34:** D354–D357

Ketela T, Green R, Bussey H (1999) Saccharomyces cerevisiae mid2p is a potential cell wall stress sensor and upstream activator of the PKC1-MPK1 cell integrity pathway. *J Bacteriol* **181:** 3330–3340

Kim KY, Truman AW, Caesar S, Schlenstedt G, Levin DE (2010) Yeast Mpk1 cell wall integrity mitogen-activated protein kinase regulates nucleocytoplasmic shuttling of the Swi6 transcriptional regulator. *Mol Biol Cell* **21:** 1609–1619

Kim KY, Truman AW, Levin DE (2008) Yeast Mpk1 mitogen-activated protein kinase activates transcription through Swi4/Swi6 by a noncatalytic mechanism that requires upstream signal. *Mol Cell Biol* **28:** 2579–2589

Kiselyov VV, Versteyhe S, Gauguin L, De Meyts P (2009) Harmonic oscillator model of the insulin and IGF1 receptors' allosteric binding and activation. *Mol Syst Biol* **5:** 243

Kitano H, Funahashi A, Matsuoka Y, Oda K (2005) Using process diagrams for the graphical representation of biological networks. *Nat Biotechnol* **23:** 961–966

Kohn KW, Aladjem MI, Kim S, Weinstein JN, Pommier Y (2006) Depicting combinatorial complexity with the molecular interaction map notation. *Mol Syst Biol* **2:** 51

Kranz JE, Satterberg B, Elion EA (1994) The MAP kinase Fus3 associates with and phosphorylates the upstream signaling component Ste5. *Genes Dev* **8:** 313–327

Kusari AB, Molina DM, Sabbagh WJr., Lau CS, Bardwell L (2004) A conserved protein interaction network involving the yeast MAP kinases Fus3 and Kss1. *J Cell Biol* **164:** 267–277

Lamson RE, Winters MJ, Pryciak PM (2002) Cdc42 regulation of kinase activity and signaling by the yeast p21-activated kinase Ste20. *Mol Cell Biol* **22:** 2939–2951

Le Novere N, Hucka M, Mi H, Moodie S, Schreiber F, Sorokin A, Demir E, Wegner K, Aladjem MI, Wimalaratne SM, Bergman FT, Gauges R, Ghazal P, Kawaji H, Li L, Matsuoka Y, Villeger A, Boyd SE, Calzone L, Courtot M *et al* (2009) The systems biology graphical notation. *Nat Biotechnol* **27:** 735–741

Le Novere N, Demir E, Mi H, Moodie S, Villeger A (2011) Systems biology graphical notation: entity relationship language Level 1 (Version 1.2). Available from Nature Precedings (http://dx.doi.org/10.1038/npre.2011.5902.1)

Lee KS, Levin DE (1992) Dominant mutations in a gene encoding a putative protein kinase (BCK1) bypass the requirement for a Saccharomyces cerevisiae protein kinase C homolog. *Mol Cell Biol* **12:** 172–182

Leeuw T, Fourest-Lieuvin A, Wu C, Chenevert J, Clark K, Whiteway M, Thomas DY, Leberer E (1995) Pheromone response in yeast: association of Bem1p with proteins of the MAP kinase cascade and actin. *Science* **270:** 1210–1213

Leeuw T, Wu C, Schrag JD, Whiteway M, Thomas DY, Leberer E (1998) Interaction of a G-protein beta-subunit with a conserved sequence in Ste20/PAK family protein kinases. *Nature* **391:** 191–195

Li E, Cismowski MJ, Stone DE (1998) Phosphorylation of the pheromone-responsive Gbeta protein of Saccharomyces cerevisiae does not affect its mating-specific signaling function. *Mol Gen Genet* **258:** 608–618

Liu K, Zhang X, Lester RL, Dickson RC (2005) The sphingoid long chain base phytosphingosine activates AGC-type protein kinases in Saccharomyces cerevisiae including Ypk1, Ypk2, and Sch9. *J Biol Chem* **280:** 22679–22687

Lok L, Brent R (2005) Automatic generation of cellular reaction networks with Moleculizer 1.0. *Nat Biotechnol* **23:** 131–136

MacKay VL, Armstrong J, Yip C, Welch S, Walker K, Osborn S, Sheppard P, Forstrom J (1991) Characterization of the Bar proteinase, an extracellular enzyme from the yeast Saccharomyces cerevisiae. *Adv Exp Med Biol* **306:** 161–172

MacKay VL, Welch SK, Insley MY, Manney TR, Holly J, Saari GC, Parker ML (1988) The Saccharomyces cerevisiae BAR1 gene encodes an exported protein with homology to pepsin. *Proc Natl Acad Sci USA* **85:** 55–59

Madden K, Sheu YJ, Baetz K, Andrews B, Snyder M (1997) SBF cell cycle regulator as a target of the yeast PKC-MAP kinase pathway. *Science* **275:** 1781–1784

Madhani HD, Fink GR (1997) Combinatorial control required for the specificity of yeast MAPK signaling. *Science* **275:** 1314–1317

Madhani HD, Styles CA, Fink GR (1997) MAP kinases with distinct inhibitory functions impart signaling specificity during yeast differentiation. *Cell* **91:** 673–684

Maeda T, Takekawa M, Saito H (1995) Activation of yeast PBS2 MAPKK by MAPKKKs or by binding of an SH3-containing osmosensor. *Science* **269:** 554–558

Maeda T, Wurgler-Murphy SM, Saito H (1994) A two-component system that regulates an osmosensing MAP kinase cascade in yeast. *Nature* **369:** 242–245

Maleri S, Ge Q, Hackett EA, Wang Y, Dohlman HG, Errede B (2004) Persistent activation by constitutive Ste7 promotes Kss1-mediated invasive growth but fails to support Fus3-dependent mating in yeast. *Mol Cell Biol* **24:** 9221–9238

Mapes J, Ota IM (2004) Nbp2 targets the Ptc1-type 2C Ser/Thr phosphatase to the HOG MAPK pathway. *EMBO J* **23:** 302–311

Martin H, Rodriguez-Pachon JM, Ruiz C, Nombela C, Molina M (2000) Regulatory mechanisms for modulation of signaling through the cell integrity Slt2-mediated pathway in Saccharomyces cerevisiae *J Biol Chem* **275:** 1511–1519

Mattison CP, Ota IM (2000) Two protein tyrosine phosphatases, Ptp2 and Ptp3, modulate the subcellular localization of the Hog1 MAP kinase in yeast. *Genes Dev* **14:** 1229–1235

Mattison CP, Spencer SS, Kresge KA, Lee J, Ota IM (1999) Differential regulation of the cell wall integrity mitogen-activated protein kinase pathway in budding yeast by the protein tyrosine phosphatases Ptp2 and Ptp3. *Mol Cell Biol* **19:** 7651–7660

Medici R, Bianchi E, Di Segni G, Tocchini-Valentini GP (1997) Efficient signal transduction by a chimeric yeast-mammalian G protein alpha subunit Gpa1-Gsalpha covalently fused to the yeast receptor Ste2. *EMBO J* **16:** 7241–7249

Melcher ML, Thorner J (1996) Identification and characterization of the CLK1 gene product, a novel CaM kinase-like protein kinase from the yeast Saccharomyces cerevisiae. *J Biol Chem* **271:** 29958–29968

Metodiev MV, Matheos D, Rose MD, Stone DE (2002) Regulation of MAPK function by direct interaction with the mating-specific Galpha in yeast. *Science* **296:** 1483–1486

Miyajima I, Nakafuku M, Nakayama N, Brenner C, Miyajima A, Kaibuchi K, Arai K, Kaziro Y, Matsumoto K (1987) GPA1, a haploid-specific essential gene, encodes a yeast homolog of mammalian G protein which may be involved in mating factor signal transduction. *Cell* **50:** 1011–1019

Murakami Y, Tatebayashi K, Saito H (2008) Two adjacent docking sites in the yeast Hog1 mitogen-activated protein (MAP) kinase differentially interact with the Pbs2 MAP kinase kinase and the Ptp2 protein tyrosine phosphatase. *Mol Cell Biol* **28:** 2481–2494

Nasmyth K, Dirick L (1991) The role of SWI4 and SWI6 in the activity of G1 cyclins in yeast. *Cell* **66:** 995–1013

Nehlin JO, Carlberg M, Ronne H (1992) Yeast SKO1 gene encodes a bZIP protein that binds to the CRE motif and acts as a repressor of transcription. *Nucleic Acids Res* **20:** 5271–5278

Neiman AM, Herskowitz I (1994) Reconstitution of a yeast protein kinase cascade in vitro: activation of the yeast MEK homologue STE7 by STE11. *Proc Natl Acad Sci USA* **91:** 3398–3402

Nern A, Arkowitz RA (1998) A GTP-exchange factor required for cell orientation. *Nature* **391:** 195–198

Nern A, Arkowitz RA (1999) A Cdc24p-Far1p-Gbetagamma protein complex required for yeast orientation during mating. *J Cell Biol* **144:** 1187–1202

Nonaka H, Tanaka K, Hirano H, Fujiwara T, Kohno H, Umikawa M, Mino A, Takai Y (1995) A downstream target of RHO1 small GTP-binding protein is PKC1, a homolog of protein kinase C, which leads to activation of the MAP kinase cascade in Saccharomyces cerevisiae. *EMBO J* **14:** 5931–5938

Olson KA, Nelson C, Tai G, Hung W, Yong C, Astell C, Sadowski I (2000) Two regulators of Ste12p inhibit pheromone-responsive transcription by separate mechanisms. *Mol Cell Biol* **20:** 4199–4209

Ostrander DB, Gorman JA (1999) The extracellular domain of the Saccharomyces cerevisiae Sln1p membrane osmolarity sensor is necessary for kinase activity. *J Bacteriol* **181:** 2527–2534

Overington J (2009) ChEMBL. An interview with John Overington, team leader, chemogenomics at the European Bioinformatics Institute Outstation of the European Molecular Biology Laboratory (EMBL-EBI). Interview by Wendy A. Warr. *J Comput Aided Mol Des* **23:** 195–198

Ozaki K, Tanaka K, Imamura H, Hihara T, Kameyama T, Nonaka H, Hirano H, Matsuura Y, Takai Y (1996) Rom1p and Rom2p are GDP/GTP exchange proteins (GEPs) for the Rho1p small GTP binding protein in Saccharomyces cerevisiae. *EMBO J* **15:** 2196–2207

Paravicini G, Friedli L (1996) Protein-protein interactions in the yeast PKC1 pathway: Pkc1p interacts with a component of the MAP kinase cascade. *Mol Gen Genet* **251:** 682–691

Parnell SC, Marotti LAJr., Kiang L, Torres MP, Borchers CH, Dohlman HG (2005) Phosphorylation of the RGS protein Sst2 by the MAP kinase Fus3 and use of Sst2 as a model to analyze determinants of substrate sequence specificity. *Biochemistry* **44:** 8159–8166

Pascual-Ahuir A, Posas F, Serrano R, Proft M (2001) Multiple levels of control regulate the yeast cAMP-response element-binding protein repressor Sko1p in response to stress. *J Biol Chem* **276:** 37373–37378

Peter M, Neiman AM, Park HO, van Lohuizen M, Herskowitz I (1996) Functional analysis of the interaction between the small GTP binding protein Cdc42 and the Ste20 protein kinase in yeast. *EMBO J* **15:** 7046–7059

Peterson J, Zheng Y, Bender L, Myers A, Cerione R, Bender A (1994) Interactions between the bud emergence proteins Bem1p and Bem2p and Rho-type GTPases in yeast. *J Cell Biol* **127:** 1395–1406

Philip B, Levin DE (2001) Wsc1 and Mid2 are cell surface sensors for cell wall integrity signaling that act through Rom2, a guanine nucleotide exchange factor for Rho1. *Mol Cell Biol* **21:** 271–280

Posas F, Saito H (1997) Osmotic activation of the HOG MAPK pathway via Ste11p MAPKKK: scaffold role of Pbs2p MAPKK. *Science* **276:** 1702–1705

Posas F, Saito H (1998) Activation of the yeast SSK2 MAP kinase kinase kinase by the SSK1 two-component response regulator. *EMBO J* **17:** 1385–1394

Posas F, Witten EA, Saito H (1998) Requirement of STE50 for osmostress-induced activation of the STE11 mitogen-activated protein kinase kinase kinase in the high-osmolarity glycerol response pathway. *Mol Cell Biol* **18:** 5788–5796

Posas F, Wurgler-Murphy SM, Maeda T, Witten EA, Thai TC, Saito H (1996) Yeast HOG1 MAP kinase cascade is regulated by a multistep phosphorelay mechanism in the SLN1-YPD1-SSK1 'two-component' osmosensor. *Cell* **86:** 865–875

Proft M, Gibbons FD, Copeland M, Roth FP, Struhl K (2005) Genomewide identification of Sko1 target promoters reveals a regulatory network that operates in response to osmotic stress in Saccharomyces cerevisiae. *Eukaryot Cell* **4:** 1343–1352

Proft M, Pascual-Ahuir A, de Nadal E, Arino J, Serrano R, Posas F (2001) Regulation of the Sko1 transcriptional repressor by the Hog1 MAP kinase in response to osmotic stress. *EMBO J* **20:** 1123–1133

Proft M, Serrano R (1999) Repressors and upstream repressing sequences of the stress-regulated ENA1 gene in Saccharomyces cerevisiae: bZIP protein Sko1p confers HOG-dependent osmotic regulation. *Mol Cell Biol* **19:** 537–546

Proft M, Struhl K (2002) Hog1 kinase converts the Sko1-Cyc8-Tup1 repressor complex into an activator that recruits SAGA and SWI/SNF in response to osmotic stress. *Mol Cell* **9:** 1307–1317

PSICQUIChttp://www.ebi.ac.uk/Tools/webservices/psicquic/view/main.xhtml

Raicu V, Jansma DB, Miller RJ, Friesen JD (2005) Protein interaction quantified in vivo by spectrally resolved fluorescence resonance energy transfer. *Biochem J* **385:** 265–277

Raitt DC, Posas F, Saito H (2000) Yeast Cdc42 GTPase and Ste20 PAK-like kinase regulate Sho1-dependent activation of the Hog1 MAPK pathway. *EMBO J* **19:** 4623–4631

Rajavel M, Philip B, Buehrer BM, Errede B, Levin DE (1999) Mid2 is a putative sensor for cell integrity signaling in Saccharomyces cerevisiae. *Mol Cell Biol* **19:** 3969–3976

Reiser V, Salah SM, Ammerer G (2000) Polarized localization of yeast Pbs2 depends on osmostress, the membrane protein Sho1 and Cdc42. *Nat Cell Biol* **2:** 620–627

Remenyi A, Good MC, Bhattacharyya RP, Lim WA (2005) The role of docking interactions in mediating signaling input, output, and discrimination in the yeast MAPK network. *Mol Cell* **20:** 951–962

Rep M, Krantz M, Thevelein JM, Hohmann S (2000) The transcriptional response of Saccharomyces cerevisiae to osmotic shock. Hot1p and Msn2p/Msn4p are required for the induction of subsets of high osmolarity glycerol pathway-dependent genes *J Biol Chem* **275:** 8290–8300

Rep M, Reiser V, Gartner U, Thevelein JM, Hohmann S, Ammerer G, Ruis H (1999) Osmotic stress-induced gene expression in Saccharomyces cerevisiae requires Msn1p and the novel nuclear factor Hot1p. *Mol Cell Biol* **19:** 5474–5485

Roberts RL, Fink GR (1994) Elements of a single MAP kinase cascade in Saccharomyces cerevisiae mediate two developmental programs in the same cell type: mating and invasive growth. *Genes Dev* **8:** 2974–2985

Schmelzle T, Helliwell SB, Hall MN (2002) Yeast protein kinases and the RHO1 exchange factor TUS1 are novel components of the cell integrity pathway in yeast. *Mol Cell Biol* **22:** 1329–1339

Schmidt A, Bickle M, Beck T, Hall MN (1997) The yeast phosphatidylinositol kinase homolog TOR2 activates RHO1 and RHO2 via the exchange factor ROM2. *Cell* **88:** 531–542

Schmidt A, Schmelzle T, Hall MN (2002) The RHO1-GAPs SAC7, BEM2 and BAG7 control distinct RHO1 functions in Saccharomyces cerevisiae. *Mol Microbiol* **45:** 1433–1441

Schmitz HP, Lorberg A, Heinisch JJ (2002) Regulation of yeast protein kinase C activity by interaction with the small GTPase Rho1p through its amino-terminal HR1 domain. *Mol Microbiol* **44:** 829–840

Shi C, Shin YO, Hanson J, Cass B, Loewen MC, Durocher Y (2005) Purification and characterization of a recombinant G-protein-coupled receptor, Saccharomyces cerevisiae Ste2p, transiently expressed in HEK293 EBNA1 cells. *Biochemistry* **44:** 15705–15714

Shimada Y, Wiget P, Gulli MP, Bi E, Peter M (2004) The nucleotide exchange factor Cdc24p may be regulated by auto-inhibition. *EMBO J* **23:** 1051–1062

Sidorova J, Breeden L (1993) Analysis of the SWI4/SWI6 protein complex, which directs G1/S-specific transcription in Saccharomyces cerevisiae. *Mol Cell Biol* **13:** 1069–1077

Siegmund RF, Nasmyth KA (1996) The Saccharomyces cerevisiae Start-specific transcription factor Swi4 interacts through the ankyrin repeats with the mitotic Clb2/Cdc28 kinase and through its conserved carboxy terminus with Swi6. *Mol Cell Biol* **16:** 2647–2655

Siekhaus DE, Drubin DG (2003) Spontaneous receptor-independent heterotrimeric G-protein signalling in an RGS mutant. *Nat Cell Biol* **5:** 231–235

Simon MN, De Virgilio C, Souza B, Pringle JR, Abo A, Reed SI (1995) Role for the Rho-family GTPase Cdc42 in yeast mating-pheromone signal pathway. *Nature* **376:** 702–705

Skowyra D, Craig KL, Tyers M, Elledge SJ, Harper JW (1997) F-box proteins are receptors that recruit phosphorylated substrates to the SCF ubiquitin-ligase complex. *Cell* **91:** 209–219

Smith GR, Givan SA, Cullen P, Sprague GFJr. (2002) GTPase-activating proteins for Cdc42. *Eukaryot Cell* **1:** 469–480

Sneddon MW, Faeder JR, Emonet T (2011) Efficient modeling, simulation and coarse-graining of biological complexity with NFsim. *Nat Methods* **8:** 177–183

Soler M, Plovins A, Martin H, Molina M, Nombela C (1995) Characterization of domains in the yeast MAP kinase Slt2 (Mpk1) required for functional activity and in vivo interaction with protein kinases Mkk1 and Mkk2. *Mol Microbiol* **17:** 833–842

Song J, Hirschman J, Gunn K, Dohlman HG (1996) Regulation of membrane and subunit interactions by N-myristoylation of a G protein alpha subunit in yeast. *J Biol Chem* **271:** 20273–20283

Stark C, Breitkreutz BJ, Reguly T, Boucher L, Breitkreutz A, Tyers M (2006) BioGRID: a general repository for interaction datasets. *Nucleic Acids Res* **34:** D535–D539

Taba MR, Muroff I, Lydall D, Tebb G, Nasmyth K (1991) Changes in a SWI4,6-DNA-binding complex occur at the time of HO gene activation in yeast. *Genes Dev* **5:** 2000–2013

Takahashi S, Pryciak PM (2007) Identification of novel membrane-binding domains in multiple yeast Cdc42 effectors. *Mol Biol Cell* **18:** 4945–4956

Tao W, Malone CL, Ault AD, Deschenes RJ, Fassler JS (2002) A cytoplasmic coiled-coil domain is required for histidine kinase activity of the yeast osmosensor, SLN1. *Mol Microbiol* **43:** 459–473

Tarassov K, Messier V, Landry CR, Radinovic S, Serna Molina MM, Shames I, Malitskaya Y, Vogel J, Bussey H, Michnick SW (2008) An in vivo map of the yeast protein interactome. *Science* **320:** 1465–1470

Tatebayashi K, Takekawa M, Saito H (2003) A docking site determining specificity of Pbs2 MAPKK for Ssk2/Ssk22 MAPKKKs in the yeast HOG pathway. *EMBO J* **22:** 3624–3634

Tatebayashi K, Tanaka K, Yang HY, Yamamoto K, Matsushita Y, Tomida T, Imai M, Saito H (2007) Transmembrane mucins Hkr1 and Msb2 are putative osmosensors in the SHO1 branch of yeast HOG pathway. *EMBO J* **26:** 3521–3533

Tatebayashi K, Yamamoto K, Tanaka K, Tomida T, Maruoka T, Kasukawa E, Saito H (2006) Adaptor functions of Cdc42, Ste50, and Sho1 in the yeast osmoregulatory HOG MAPK pathway. *EMBO J* **25:** 3033–3044

Tedford K, Kim S, Sa D, Stevens K, Tyers M (1997) Regulation of the mating pheromone and invasive growth responses in yeast by two MAP kinase substrates. *Curr Biol* **7:** 228–238

Thorner J, Westfall PJ, Ballon DR (2005) High Osmolarity Glycerol (HOG) pathway in yeast. *Sci. Signal* (Connections Map in the Database of Cell Signaling, as seen 10 January 2011) http://stke.sciencemag.org/cgi/cm/stkecm;CMP_14620

Truckses DM, Bloomekatz JE, Thorner J (2006) The RA domain of Ste50 adaptor protein is required for delivery of Ste11 to the plasma membrane in the filamentous growth signaling pathway of the yeast Saccharomyces cerevisiae. *Mol Cell Biol* **26:** 912–928

Truman AW, Kim KY, Levin DE (2009) Mechanism of Mpk1 mitogen-activated protein kinase binding to the Swi4 transcription factor and its regulation by a novel caffeine-induced phosphorylation. *Mol Cell Biol* **29:** 6449–6461

Vadaie N, Dionne H, Akajagbor DS, Nickerson SR, Krysan DJ, Cullen PJ (2008) Cleavage of the signaling mucin Msb2 by the aspartyl protease Yps1 is required for MAPK activation in yeast. *J Cell Biol* **181:** 1073–1081

Valtz N, Peter M, Herskowitz I (1995) FAR1 is required for oriented polarization of yeast cells in response to mating pheromones. *J Cell Biol* **131:** 863–873

Varanasi US, Klis M, Mikesell PB, Trumbly RJ (1996) The Cyc8 (Ssn6)-Tup1 corepressor complex is composed of one Cyc8 and four Tup1 subunits. *Mol Cell Biol* **16:** 6707–6714

Verna J, Lodder A, Lee K, Vagts A, Ballester R (1997) A family of genes required for maintenance of cell wall integrity and for the stress response in Saccharomyces cerevisiae. *Proc Natl Acad Sci USA* **94:** 13804–13809

Vilella F, Herrero E, Torres J, de la Torre-Ruiz MA (2005) Pkc1 and the upstream elements of the cell integrity pathway in Saccharomyces cerevisiae, Rom2 and Mtl1, are required for cellular responses to oxidative stress. *J Biol Chem* **280:** 9149–9159

Wang HX, Konopka JB (2009) Identification of amino acids at two dimer interface regions of the alpha-factor receptor (Ste2). *Biochemistry* **48:** 7132–7139

Wang Y, Chen W, Simpson DM, Elion EA (2005) Cdc24 regulates nuclear shuttling and recruitment of the Ste5 scaffold to a heterotrimeric G protein in Saccharomyces cerevisiae. *J Biol Chem* **280:** 13084–13096

Warmka J, Hanneman J, Lee J, Amin D, Ota I (2001) Ptc1, a type 2C Ser/Thr phosphatase, inactivates the HOG pathway by dephosphorylating the mitogen-activated protein kinase Hog1. *Mol Cell Biol* **21:** 51–60

Wassmann K, Ammerer G (1997) Overexpression of the G1-cyclin gene CLN2 represses the mating pathway in Saccharomyces cerevisiae at the level of the MEKK Ste11. *J Biol Chem* **272:** 13180–13188

Watanabe M, Chen CY, Levin DE (1994) Saccharomyces cerevisiae PKC1 encodes a protein kinase C (PKC) homolog with a substrate specificity similar to that of mammalian PKC. *J Biol Chem* **269:** 16829–16836

Watanabe Y, Irie K, Matsumoto K (1995) Yeast RLM1 encodes a serum response factor-like protein that may function downstream of the Mpk1 (Slt2) mitogen-activated protein kinase pathway. *Mol Cell Biol* **15:** 5740–5749

Watanabe Y, Takaesu G, Hagiwara M, Irie K, Matsumoto K (1997) Characterization of a serum response factor-like protein in Saccharomyces cerevisiae, Rlm1, which has transcriptional activity regulated by the Mpk1 (Slt2) mitogen-activated protein kinase pathway. *Mol Cell Biol* **17:** 2615–2623

Winters MJ, Pryciak PM (2005) Interaction with the SH3 domain protein Bem1 regulates signaling by the Saccharomyces cerevisiae p21-activated kinase Ste20. *Mol Cell Biol* **25:** 2177–2190

Wu C, Jansen G, Zhang J, Thomas DY, Whiteway M (2006) Adaptor protein Ste50p links the Ste11p MEKK to the HOG pathway through plasma membrane association. *Genes Dev* **20:** 734–746

Wu C, Leberer E, Thomas DY, Whiteway M (1999) Functional characterization of the interaction of Ste50p with Ste11p MAPKKK in Saccharomyces cerevisiae. *Mol Biol Cell* **10:** 2425–2440

Wu C, Whiteway M, Thomas DY, Leberer E (1995) Molecular characterization of Ste20p, a potential mitogen-activated protein or extracellular signal-regulated kinase kinase (MEK) kinase kinase from Saccharomyces cerevisiae. *J Biol Chem* **270:** 15984–15992

Wu YL, Hooks SB, Harden TK, Dohlman HG (2004) Dominant-negative inhibition of pheromone receptor signaling by a single point mutation in the G protein alpha subunit. *J Biol Chem* **279:** 35287–35297

Wurgler-Murphy SM, Maeda T, Witten EA, Saito H (1997) Regulation of the Saccharomyces cerevisiae HOG1 mitogen-activated protein kinase by the PTP2 and PTP3 protein tyrosine phosphatases. *Mol Cell Biol* **17:** 1289–1297

Xenarios I, Salwinski L, Duan XJ, Higney P, Kim SM, Eisenberg D (2002) DIP, the Database of Interacting Proteins: a research tool for studying cellular networks of protein interactions. *Nucleic Acids Res* **30:** 303–305

Yablonski D, Marbach I, Levitzki A (1996) Dimerization of Ste5, a mitogen-activated protein kinase cascade scaffold protein, is required for signal transduction. *Proc Natl Acad Sci USA* **93:** 13864–13869

Yamamoto K, Tatebayashi K, Tanaka K, Saito H (2010) Dynamic control of yeast MAP kinase network by induced association and dissociation between the Ste50 scaffold and the Opy2 membrane anchor. *Mol Cell* **40:** 87–98

Yang J, Meng X, Hlavacek WS (2010) *Rule-based Modeling and Simulation of Biochemical Systems with Molecular Finite Automata* **23**
yeastpheromonemodel.org

Yesilaltay A, Jenness DD (2000) Homo-oligomeric complexes of the yeast alpha-factor pheromone receptor are functional units of endocytosis. *Mol Biol Cell* **11:** 2873–2884

Young C, Mapes J, Hanneman J, Al-Zarban S, Ota I (2002) Role of Ptc2 type 2C Ser/Thr phosphatase in yeast high-osmolarity glycerol pathway inactivation. *Eukaryot Cell* **1:** 1032–1040

Yuan YL, Fields S (1991) Properties of the DNA-binding domain of the Saccharomyces cerevisiae STE12 protein. *Mol Cell Biol* **11:** 5910–5918

Zarrinpar A, Bhattacharyya RP, Nittler MP, Lim WA (2004) Sho1 and Pbs2 act as coscaffolds linking components in the yeast high osmolarity MAP kinase pathway. *Mol Cell* **14:** 825–832

Zarrinpar A, Park SH, Lim WA (2003) Optimization of specificity in a cellular protein interaction network by negative selection. *Nature* **426:** 676–680

Zarzov P, Mazzoni C, Mann C (1996) The SLT2(MPK1) MAP kinase is activated during periods of polarized cell growth in yeast. *EMBO J* **15:** 83–91

Zeitlinger J, Simon I, Harbison CT, Hannett NM, Volkert TL, Fink GR, Young RA (2003) Program-specific distribution of a transcription factor dependent on partner transcription factor and MAPK signaling. *Cell* **113:** 395–404

Zhan XL, Deschenes RJ, Guan KL (1997) Differential regulation of FUS3 MAP kinase by tyrosine-specific phosphatases PTP2/PTP3 and dual-specificity phosphatase MSG5 in Saccharomyces cerevisiae. *Genes Dev* **11:** 1690–1702

Zhan XL, Guan KL (1999) A specific protein-protein interaction accounts for the in vivo substrate selectivity of Ptp3 towards the Fus3 MAP kinase. *Genes Dev* **13:** 2811–2827

Zhao ZS, Leung T, Manser E, Lim L (1995) Pheromone signalling in Saccharomyces cerevisiae requires the small GTP-binding protein Cdc42p and its activator CDC24. *Mol Cell Biol* **15:** 5246–5257

Zheng CF, Guan KL (1994) Activation of MEK family kinases requires phosphorylation of two conserved Ser/Thr residues. *EMBO J* **13:** 1123–1131

Zheng Y, Cerione R, Bender A (1994) Control of the yeast bud-site assembly GTPase Cdc42. Catalysis of guanine nucleotide exchange by Cdc24 and stimulation of GTPase activity by Bem3. *J Biol Chem* **269:** 2369–2372

Zhou Z, Gartner A, Cade R, Ammerer G, Errede B (1993) Pheromone-induced signal transduction in Saccharomyces cerevisiae requires the sequential function of three protein kinases. *Mol Cell Biol* **13:** 2069–2080